

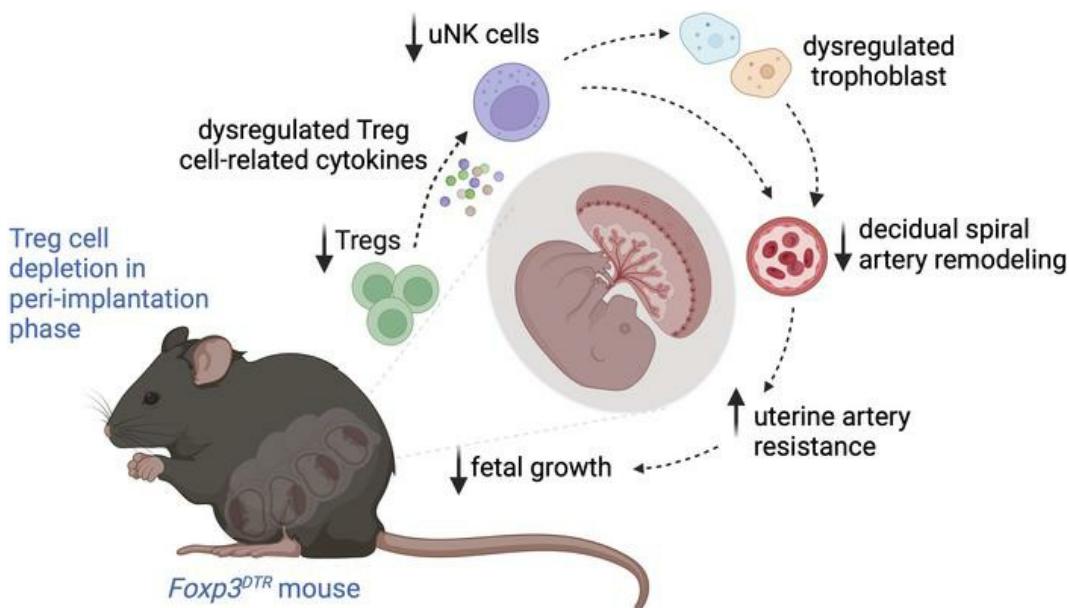
Regulatory T cells promote decidual vascular remodeling and modulate uterine NK cells in pregnant mice

Shanna L. Hosking, ... , Sarah A. Robertson, Alison S. Care

JCI Insight. 2024. <https://doi.org/10.1172/jci.insight.169836>.

Research In-Press Preview Immunology Reproductive biology

Graphical abstract



Find the latest version:

<https://jci.me/169836/pdf>



1 **Regulatory T cells promote decidual vascular remodeling and modulate**
2 **uterine NK cells in pregnant mice**

3

4 Shanna L. Hosking¹, Lachlan M. Moldenhauer¹, Ha M. Tran¹, Hon Y. Chan¹, Holly M. Groome¹,
5 Evangeline A. K. Lovell¹, Ella S. Green¹, Stephanie E. O'Hara¹, Claire T. Roberts², Kerrie L.
6 Foyle¹, Sandra T. Davidge³, Sarah A. Robertson^{1*}, Alison S. Care^{1*}

7

8 ¹Robinson Research Institute and School of Biomedicine, The University of Adelaide, Adelaide,
9 SA, 5000, Australia

10 ²Flinders Health and Medical Research Institute, Flinders University, Adelaide, SA 5042,
11 Australia.

12 ³Women and Children's Health Research Institute, Department of Obstetrics and Gynaecology,
13 University of Alberta, Edmonton, AB, T6G 2S2, Canada

14

15 *ASC and SAR are co-senior authors

16

17 Address correspondence to: Dr Alison S. Care, Robinson Research Institute and School of
18 Biomedicine, The University of Adelaide, South Australia, 5000, Australia.

19 Ph: +61 883131504. Email: alison.care@adelaide.edu.au

20

21 Conflict of interest statement: The authors have declared that no conflict of interest exists.

22

23

24

25 **ABSTRACT**

26 Regulatory T (Treg) cells are essential for maternal immune tolerance of the fetus and placenta. In
27 preeclampsia, aberrant Treg cell tolerance is implicated, but whether and how Treg cells affect the
28 uterine vascular dysfunction thought to precede placental impairment and maternal vasculopathy
29 is unclear. We utilized *Foxp3^{DTR}* mice to test the hypothesis that Treg cells are essential regulators
30 of decidual spiral artery adaptation to pregnancy. Transient Treg cell depletion during early
31 placental morphogenesis caused impaired remodeling of decidual spiral arteries, altered uterine
32 artery function and led to fewer DBA⁺ uterine natural killer (uNK) cells, resulting in late gestation
33 fetal loss and fetal growth restriction. Replacing the Treg cells by transfer from wild-type donors
34 mitigated the impact on uNK cells, vascular remodeling, and fetal loss. RNA sequencing of
35 decidua revealed genes associated with NK cell function and placental extravillous trophoblasts
36 were dysregulated after Treg cell depletion, and normalized by Treg cell replacement. These data
37 implicate Treg cells as essential upstream drivers of uterine vascular adaptation to pregnancy,
38 through a mechanism likely involving phenotypic regulation of uNK cells and trophoblast
39 invasion. The findings provide insight into mechanisms linking impaired adaptive immune
40 tolerance and altered spiral artery remodeling, two hallmark features of preeclampsia.

41

42

43 **INTRODUCTION**

44 Regulatory T (Treg) cells are a specialized subset of T cells that suppress inflammation and limit
45 deleterious immune responses to self and foreign antigens (1). Treg cells have a pivotal role in
46 immune homeostasis by modulating the proliferation and activity of effector T and B cells, and
47 natural killer (NK) cells. Treg cells are essential for pregnancy tolerance; sufficient numbers of
48 functionally competent Treg cells must be present in the uterus for successful embryo implantation
49 and placental development (2). Since pregnancy is an inflammatory state and the fetoplacental unit
50 expresses paternally-derived alloantigens (2), the uterine Treg cell pool has important roles in
51 constraining inflammation and preventing aberrant maternal immune reactivity (3-6).

52

53 Fewer or functionally impaired Treg cells are a common feature of preeclampsia (7-11)—a serious
54 hypertensive disorder that affects 2-8% of all pregnant women (12, 13). Treg cell deficiency
55 associated with aberrant generation of effector T(eff) cells, including pro-inflammatory Th1 and
56 Th17 cells (8, 14), is evident in peripheral blood and uterine decidual tissue in preeclampsia (7-
57 11), and may originate due to insufficient priming towards paternal alloantigens and/or underlying
58 immune dysfunction (15). Although a definitive causal role for Treg cell deficiency in the placental
59 pathophysiology of these conditions is not proven in humans, studies in rodent models (16, 17)
60 indicate biological plausibility and the significance of paternal factors is consistent with a
61 maladaptive immune response (15, 18).

62

63 One candidate mechanism by which Treg cell insufficiency may contribute to defective
64 placentation involves the uterine blood supply (19). Emerging evidence shows Treg cells are
65 essential regulators of systemic vascular homeostasis supporting healthy cardiovascular function

66 in a range of tissues (20, 21). Treg cell insufficiency has been linked to hypertension and aberrant
67 vascular remodeling (22, 23), while treatment interventions to boost Treg cells can reverse
68 cardiovascular dysfunction (24, 25) and mitigate hypertension (24). These considerations raise the
69 prospect that in addition to their immune regulatory roles, Treg cells might facilitate the vascular
70 adaptations required to accommodate pregnancy – but whether and how this occurs is unknown.

71

72 The maternal cardiovascular system must undergo substantial remodeling to support pregnancy
73 and enable optimal placental function. These events commence with local changes to the uterine
74 vasculature during early placental development. Systemic cardiovascular adaptations follow,
75 featuring increased blood volume, enhanced cardiac output, and reduced total peripheral resistance
76 (26). A substantial increase in blood supply to the uterine artery and the placenta supports the
77 increasing nutrient demands of the developing fetus as gestation proceeds (27). Robust fetal
78 growth in late gestation therefore depends on adequate early remodeling and vasodilation of the
79 uterine artery and its network of decidual spiral arteries (27-29).

80

81 Decidual spiral arteries are the terminal branch of the main uterine arteries. Their remodeling
82 involves trophoblast invasion of the decidual vessel wall and a loss of the surrounding smooth
83 muscle cells and elastic lamina in women (30), with similar features during placentation in mice
84 (31). Migrating extravillous trophoblast cells invade both the decidual interstitium and the
85 endovascular space within the spiral arteries to facilitate their transformation from high-resistance
86 vessels to low-resistance, high-capacity vessels. These vessels perfuse the placental intervillous
87 space from which exchange of nutrients and oxygen between maternal and fetal circulations occurs
88 (32) to accommodate escalating fetal demand as pregnancy progresses (33).

89

90 Immune cells, particularly uterine natural killer (uNK) cells, are critical for decidual spiral artery
91 remodeling (34). uNKs are an abundant subset of innate lymphoid cells in the decidua (35) that
92 are essential for decidual vascular remodeling in mice (34, 36, 37), and humans (38). They secrete
93 cytokines such as IFN γ and VEGFA (35, 37, 39, 40) and enzymes that modulate endothelial cell
94 tight junctions, cause smooth muscle cell apoptosis, and promote trophoblast invasion (34, 41).
95 Elevated inflammatory activity impairs uNK cell function, leading to shallow spiral artery
96 remodeling and placental dysfunction (42, 43).

97

98 We previously demonstrated that depletion of Treg cells from pregnant mice causes dysfunction
99 in the main arteries serving the uterus, causing increased resistance and altered regulation of
100 vasoconstriction, in turn affecting systemic blood pressure regulation (19). Additionally, we
101 showed Treg cell deficiency caused by insufficient progesterone signaling elicits impaired
102 decidual spiral artery remodeling (16), building on other studies noting that Treg cell perturbation
103 can be accompanied by uterine vascular changes (2, 19, 44). However, there has been no formal
104 investigation of the specific requirement for Treg cells in remodelling of the decidual spiral arteries
105 or investigation of the cellular mechanisms by which this might occur.

106

107 In this study, we test the hypothesis that Treg cells are essential for decidual spiral artery
108 remodeling in early pregnancy, utilizing *Foxp3*^{DTR} transgenic mice (45) to allow acute, transient
109 Treg cell depletion. Here we report evidence that Treg cell deficiency is a primary cause of poor
110 remodeling of decidual spiral arteries, causing fetal loss and growth restriction in surviving fetuses,
111 and a mechanism involving dysregulation of uNK cells and altered trophoblast invasion is

112 implicated. Our data provide compelling evidence to link Treg cells and uteroplacental vascular
113 remodeling in an interactive network underpinning establishment and progression of healthy
114 pregnancy.

115

116 **RESULTS**

117 *Treg cell depletion during the peri-implantation period causes fetal loss and fetal growth*
118 *restriction*

119 To evaluate the physiological significance of Treg cells in the peri-implantation phase for
120 pregnancy progression, we administered DT on gestational day (GD)3.5 and 5.5 to selectively and
121 transiently deplete the Treg cell pool, as previously described (19). In *Foxp3^{DTR}* mice treated with
122 DT, Treg cells (measured as a proportion of CD4⁺ T cells) were reduced by $\geq 97\%$ in the uterine-
123 draining, para-aortic lymph nodes (uDLN) by GD6.5, 24 h post-treatment. This site is where Treg
124 cells normally proliferate prior to recruitment into the uterus (46)(Figure 1A, B). In contrast, Treg
125 cells in vehicle-treated control *Foxp3^{DTR}* mice remained unchanged. Analysis at the critical mid-
126 gestation timepoint of GD10.5, when the mouse placenta is mature and placental access to the
127 maternal blood supply is complete (30, 47), showed partial repopulation of Treg cells in the uDLN,
128 although their proportion remained $\sim 59\%$ less than in control mice (Figure 1B). The majority of
129 Treg cells in the uDLN in mid-gestation were thymic-derived as indicated by NRP1 expression
130 (48), regardless of earlier Treg cell depletion (Figure 1C). Repopulating Treg cells more commonly
131 expressed the proliferation marker Ki67 (Figure 1D), while similar proportions expressed CTLA4,
132 a marker of suppressive competence (49)(Figure 1E). Treg cell deficiency did not cause an increase
133 in CD4⁺ T cell expression of IFN γ or IL17a (Figure 1F, G). Comparable effects were seen in the
134 spleen, consistent with a systemic impact of DT on Treg cells in *Foxp3^{DTR}* mice (Supplemental
135 Figure 1). Recovery was faster in the spleen, such that on GD10.5 Treg cells were not different in
136 proportion or phenotype between DT-treated and control mice (Supplemental Figure 1A-D), and
137 IFN γ and IL17a expression were unchanged (Supplemental Figure 1E, F).

138

139 To evaluate the impact of peri-implantation pregnancy Treg cell depletion on pregnancy success,
140 *Foxp3*^{DTR} mice were given DT or vehicle control and birth outcomes were recorded. Additional
141 groups of DT-treated *Foxp3*^{DTR} mice were administered wild-type Treg cells (CD4⁺CD25⁺ cells)
142 that do not express human DTR and are refractive to DT-induced depletion (45), or conventional
143 CD4⁺ T cells (Tconv; CD4⁺CD25⁻ cells), on GD2.5 and GD4.5. Transferred cells were prepared
144 from the spleens and lymph nodes of pregnant donor mice to ensure hormone and antigen priming,
145 which are important for Treg cell function in pregnancy (50). A subset of dams were allowed to
146 give birth and birth outcomes were evaluated, and for another subset, pregnancy outcomes were
147 evaluated in late gestation (Figure 2A).

148

149 Compared to control dams administered vehicle, Treg cell depletion compromised pup viability at
150 birth (Figure 2D, E) and reduced pup weight (Figure 2F), but had no impact on the proportion of
151 dams with viable pregnancies (defined as 1 or more viable pup), or total pups born (Figure 2B, C).
152 Pre-treatment with wild-type Treg cells in DT-treated *Foxp3*^{DTR} mice prevented the shift in
153 pregnancy success, litter size and birth weight, while Tconv cells did not confer the same
154 improvement (Figure 2D-F).

155

156 The poor pregnancy outcomes after peri-implantation Treg cell depletion prompted us to evaluate
157 late gestation fetal and placental parameters. In DT-treated and vehicle control *Foxp3*^{DTR} mice
158 autopsied at GD18.5, the rate of viable pregnancy (defined as at least one viable fetus), and total
159 or viable implantation sites per dam (Figure 2G-I) were unchanged. However, DT treatment caused
160 an increase in both the number and the proportion of overt fetal losses (resorptions) per dam
161 compared to control mice (Figure 2J-K), indicating fetal loss occurred after mid-gestation. Pre-

162 treatment with wild-type Treg cells mitigated against Treg cell deficiency (Figure 2J, K), such that
163 resorptions were not different to control mice. In contrast, Tconv cells did not attenuate the effects
164 of Treg cell deficiency (Figure 2J, K).

165

166 Surviving fetuses from *Foxp3^{DTR}* mice treated with DT to elicit Treg cell depletion were growth
167 restricted on GD18.5, compared to vehicle-treated controls. Fetal weight was reduced by 3.1%,
168 crown-to-rump length by 1.9%, abdominal girth by 3.4%, and biparietal diameter by 5.0% (Figure
169 3A, B, H-J). Transfer of wild-type Treg cells to DT-treated mice did not correct late-gestation fetal
170 weight (Figure 3B) but did mitigate other parameters of fetal growth (Figure 3H-J). In contrast,
171 Tconv cells further reduced fetal weight, crown-to-rump length, and biparietal diameter (Figure
172 3B, H, J). When fetal weight distribution was considered (Figure 3E), 27% were below the 10th
173 percentile in DT-treated mice, compared to 21% in dams given DT and Treg cells, and 46% in
174 dams given DT and Tconv cells.

175

176 There was no impact of Treg cell depletion from *Foxp3^{DTR}* mice, nor exogenous Treg cell or Tconv
177 cell administration, on placental weight (Figure 3C, F). However, Treg cell depletion reduced the
178 fetal:placental weight ratio, a surrogate measure of placental efficiency (Figure 3D, G). This was
179 unchanged by Treg cell or Tconv transfer (Figure 3D). This indicates that as well as fetal loss,
180 Treg cell depletion impaired placental efficiency in surviving fetuses, in turn affecting fetal
181 growth. Together these data show that Treg cell deficiency, and not off-target effects of DT
182 treatment, are responsible for fetal loss and fetal growth impairment. Consistent with this
183 interpretation, no effect of DT on fetal survival, fetal weight, or growth parameters was seen in

184 wild-type C57BL/6 mice given DT on GD3.5 and 5.5, compared to mice given vehicle
185 (Supplemental Figure 2).

186

187 To further investigate the impacts of Treg cell depletion, placental structure was assessed in late
188 gestation (Supplemental Figure 3A-D). There was no effect of Treg cell depletion on placental
189 structure at GD18.5 as indicated by area of junctional zone (JZ) or labyrinth zone (LZ), the tissues
190 responsible for endocrine function and nutrient transfer respectively (Supplemental Figure 3E-I).
191 The proportion of glycogen cells in the junctional zone was increased following DT treatment to
192 elicit Treg cell depletion compared to control mice. This was prevented by treatment with Treg
193 cells but not Tconv cells (Supplemental Figure 3J).

194

195 *Treg cell depletion disrupts uterine vascular function and decidual spiral artery remodeling*

196 We next investigated the impact of Treg cell depletion on the uterine vasculature in mid-gestation,
197 as this is a critical determinant of placental maturation and capacity to support fetal survival and
198 growth. At GD10.5, *Foxp3*^{DTR} dams given DT to elicit Treg cell depletion had a similar rate of
199 viable pregnancy, number of total and viable implantation sites per dam, and proportion and
200 number of abnormal implantation sites showing early signs of resorption compared to vehicle-
201 treated control *Foxp3*^{DTR} dams. Transfer of Treg cells or Tconv cells did not change these
202 parameters (Supplemental Figure 4A-I).

203

204 When decidual spiral artery remodeling was quantified stereologically in midsagittal sections of
205 implantation sites on GD10.5, impaired spiral artery remodeling was seen after Treg cell depletion
206 (Figure 4A-D). Decidual spiral artery lumen area and lumen diameter were reduced by 29% and

207 15% respectively compared to control (Figure 4A-B, I-J). There was a trend towards an increased
208 relative wall thickness in decidual spiral arteries (vessel:lumen ratio) after Treg cell depletion
209 (Figure 4K; P=0.08). Transfer of wild-type Treg cells normalized decidual spiral artery remodeling
210 (Figure 4C, I-J), but Tconv cells did not (Figure 4D, I-J), and increased the relative wall thickness
211 of vessels, compared to control mice (Figure 4K).

212

213 Smooth muscle cells are normally lost from the arterial vascular media during the spiral artery
214 remodeling process, and smooth muscle actin (SMA) retention indicates impaired remodeling (51).
215 Depletion of Treg cells from *Foxp3^{DTR}* mice resulted in a 2-fold increase of SMA expression
216 compared to control *Foxp3^{DTR}* mice (Figure 4E-F, L). Loss of SMA was improved by transfer of
217 Treg cells (Figure 4G, L), but not Tconv cells (Figure 4H, L).

218

219 To determine the impact of Treg cell perturbation in the peri-implantation phase on function of the
220 main uterine arteries in mid-gestation, we used ultrasound biomicroscopy on GD9.5. Treg cell
221 depletion was found to increase uterine artery resistance index by 11.0%, indicating increased
222 resistance to blood flow (Figure 5A, B). Administration of Treg cells, but not Tconv cells,
223 mitigated the increase in uterine artery resistance (Figure 5B). Uterine artery pulsatility index,
224 another measure of resistance, showed an increasing trend following Treg cell depletion (P=0.06;
225 Figure 5C) that was partially improved by Treg cell transfer, but not Tconv cells (Figure 5C).
226 These findings build upon our previous report of altered uterine vascular parameters after Treg
227 cell depletion (19). The effect of Treg cell depletion on uterine artery function was limited to mid-
228 pregnancy – when uterine artery and umbilical artery function were measured on GD17.5, there

229 was no impact of Treg cell depletion or treatment with Treg or Tconv cells (Supplemental Table
230 1).

231

232 *Treg cell depletion modifies uNK cells, key regulators of spiral artery remodeling*

233 Given the central role of uNK cells in spiral artery remodeling, we next investigated whether uNK
234 cells contribute to the mechanism by which Treg cell deficiency causes remodeling impairment.

235 Initially, uNK cell abundance was assessed by histological staining with *Dolichos biflorus*
236 agglutinin (DBA) lectin to identify uNK cells in midsagittal sections of implantation sites. DBA

237 reacts with *N*-acetylgalactosamine (GalNAc) residues present on the cell surface and in granules
238 of uNK cells (52). DBA⁺ uNK cells, which predominate in pregnancy, produce factors including

239 VEGFA that facilitate spiral artery remodeling by promoting migration of extravillous trophoblasts
240 through the decidua (40), while DBA⁻ uNK cells produce IFN γ (35, 40). Compared to vehicle-

241 treated control *Foxp3*^{DTR} mice, Treg cell-depleted *Foxp3*^{DTR} mice had substantially less DBA
242 staining in the decidua on GD10.5 (Figure 6A, B, E). DBA⁺ uNK cell abundance was normalized

243 by Treg cell transfer, but not by Tconv cells (Figure 6A-E). Notably, the total mid-sagittal area of
244 decidual tissue was not affected by Treg cell depletion, indicating the vascular and uNK cell
245 changes were unlikely to be due to defective decidualization (Figure 6F).

246

247 To further understand the impact of Treg cell depletion, uNK cells were investigated by flow

248 cytometry. uNK cells can be classified into three subsets with distinguishing surface phenotypes
249 with potential for distinct roles in angiogenesis and vascular remodeling (53). All three subsets

250 express the NK lineage-defining surface marker NK1.1 (54) and acquire NKp46 [also termed
251 natural cytotoxicity receptor (NCR)1] upon maturation in the decidua (55-58). The uNK cell

252 subsets include: (1) tissue resident (tr)NKs, defined as CD45⁺NK1.1⁺CD11B^{lo/-}
253 NKp46⁺CD49a⁺EOMES⁺ cells; (2) conventional NK (cNK) defined as CD45⁺NK1.1⁺CD11B^{lo/-}
254 NKp46⁺CD49a⁻ cells, and (3) group 1 innate lymphoid cells (ILC1) defined as
255 CD45⁺NK1.1⁺CD11B^{lo/-}NKp46⁺CD49a⁺EOMES⁻ cells. cNK cells are the primary source of IFN γ
256 (58) while trNKs produce VEGFA. When trNK, cNK, and ILC1 cells were analyzed in decidua
257 recovered on GD10.5 from vehicle- or DT-treated *Foxp3*^{DTR} mice, as expected the largest
258 population was trNKs, followed by cNKs and then ILC1s (Supplemental Figure 5A-E (58)). Treg
259 cell depletion did not change the proportion of NK1.1⁺ uNK cells categorised as cNK, ILC1, or
260 trNK compared to vehicle-treated control mice (Supplemental Figure 5C-E). Similarly no change
261 was seen in the proportion of NK1.1⁺ or NKp46⁺ NK cells amongst non-T, non-B cells, or the total
262 CD3⁺ T cells (Supplemental Figure 5F-J).

263

264 *Transcriptomic analysis shows canonical NK cell and T cell pathways are disrupted by Treg cell*
265 *depletion and restored by Treg cell replacement.*

266 The data indicating fewer DBA⁺ uNK cells compelled us to investigate the impact of Treg cell
267 depletion on gene transcription in the decidua following Treg cell depletion. We performed RNA
268 sequencing on decidual tissue collected at GD10.5 from vehicle-treated (veh), DT-treated
269 *Foxp3*^{DTR} mice (DT), and DT-treated *Foxp3*^{DTR} mice given wild-type Treg cells (DT+Treg; N=5-
270 6 samples per group; see Supplemental Table 2 for RNA-seq metrics). After removal of non- and
271 lowly-expressed genes, 14748 genes were TMM-normalized and subsequent dimensionality
272 reduction via principal component analysis (PCA) identified three distinct clusters corresponding
273 to the three treatment groups (Figure 7A).

274

275 Transcriptomic profiling identified 446 differentially expressed genes (DEGs) following Treg
276 depletion compared to the vehicle-treated group (DT vs veh), including 192 upregulated and 254
277 downregulated genes (all differentially expressed genes detected are listed in the Supporting Data
278 Values file, and the top 50 up- and downregulated genes are listed in Supplemental Table 3 and
279 4). In mice that received Treg cells as well as DT (DT+Treg group) the majority of the 446 DEGs
280 were unchanged and only 35 of the 446 DEGs were differentially expressed (Figure 7B), indicating
281 partial normalization of the transcriptional changes.

282
283 To understand their functional significance, over-representation analysis of the DEGs from these
284 comparisons were performed using Gene Ontology (GO) (59), Kyoto Encyclopaedia of Genes and
285 Genomes (KEGG) (60), Reactome (61), and Ingenuity Pathway Analysis (IPA, QIAGEN)
286 databases (Supplemental Figures 6-8). Pathways regulated by Treg depletion during the peri-
287 implantation phase predominantly reflected immune effector responses, particularly those
288 involving NK cell and T cell activation and cytotoxicity. Notably, GO analysis identified
289 Granzyme-Mediated Programmed Cell Death Signaling Pathway, T Cell Mediated Cytotoxicity,
290 NK Cell Mediated Cytotoxicity, and NK Cell Lectin-like Receptor Binding pathways
291 (Supplemental Figure 6), while KEGG analysis identified pathways including Graft versus Host
292 Disease, Allograft Rejection and Natural Killer Cell-mediated Cytotoxicity (Supplemental Figure
293 7). IPA revealed that Interferon Gamma Signaling and Interferon Alpha/Beta Signaling were
294 amongst the top canonical pathways (Supplemental Figure 8) and biological functions invoking
295 lymphocyte cytotoxicity (Supplemental Figure 9). The logFC of DEGs linked with selected
296 pathways associated with NK cell and T cell activation are shown in Figure 7C.

297

298 Strikingly, transfer of wild-type Treg cells to DT-treated *Foxp3*^{DTR} mice substantially normalised
299 most of the DEGs (Supplemental Table 3 and 4), including many of the DEGs annotated to NK
300 and T cell activation pathways (Figure 7C). Amongst the effector genes upregulated by Treg
301 depletion and downregulated by Treg cell replacement were genes encoding granzyme B (*Gzmb*)
302 and perforin pore-forming proteins (*Prfl*) that mediate lymphocyte cytotoxicity, as well as
303 granzymes associated with remodeling activity *Gzmc*, *Gzmd*, *Gzme*, *Gzmf*, *Gzmg* (62-64). Certain
304 NK cell-associated transcription factors were upregulated after Treg cell depletion, notably *Eomes*,
305 *Id2*, and *Runx3* which control aspects of NK cell maturation and function. Many genes involved
306 in the interferon response pathway, a key program associated with activation of cNK and ILC1
307 cells, were also upregulated, as were genes *Il15ra*, *Il2rb*, and *Il2rg* encoding the three components
308 of the trimeric IL15 receptor (IL15R α , IL15R β , and IL2R γ) that mediates uNK cell responsiveness
309 to the uNK cell activating cytokine IL15.

310

311 An extensive array of genes known to be expressed by placental trophoblasts were also present
312 among the DEGs (Supplemental Figure 10). A subset of these trophoblast genes selected on the
313 basis of their absence in uterine cells (indicating trophoblast specificity (65)) included *Cdh5*, *Lcp1*,
314 and *Olr1*, all of which are associated with placental glycogen cells (65)(Figure 8, Supplemental
315 Figure 10). Others including *Krt7*, *Krt8* *Psck6*, *Cited4*, and *Hsd11b2* expressed by various
316 extravillous trophoblast lineages (66) were downregulated in decidual tissue after Treg cell
317 depletion (Figure 8). These trophoblast genes were largely normalized after Treg cell replacement
318 (Figure 8, Supplemental Figure 10).

319

320 Notably, there was no evidence of altered expression of hallmark decidualization genes *Prl*,
321 *Igfbp1*, *Foxo1*, *Fstl1*, *Bmp2*, or *Ptgs2*, following Treg depletion as might be expected if decidual
322 development or function was compromised (Supporting Data Values file). These observations
323 clearly point to the significance of Treg cells in constraining uNK cell activation pathways under
324 normal conditions and strongly suggest a role for inappropriately activated uNK cells and altered
325 trophoblast cell invasion or survival in the observed vascular remodeling and fetal loss seen after
326 Treg cell depletion.

327

328 *Treg cell-derived anti-inflammatory cytokines are implicated in uNK cell regulation.*

329 Upstream regulator analysis in IPA was performed to identify factors implicated as potential
330 regulators of the Treg cell depletion-induced decidual gene transcription changes. The predicted
331 upstream regulators included 93 candidate immune regulatory cytokines, cytokine receptors and
332 transcription factors. Around half of these overlapped with genes detected in decidual tissue and
333 some were DEGs regulated by Treg cell depletion and replacement (Supplemental Figure 11).
334 Notably, the predicted regulators included two factors known to be released by Treg cells with
335 potential to modulate uNK cell function, IL10 (activation Z-score=2.1) and EBI3 (a subunit of
336 IL35; activation Z-score=2.6). IL35 is an immunosuppressive cytokine composed of two chains,
337 IL12 α (p35) and EBI3 (67), that is produced exclusively by Treg cells to modulate the function of
338 NK cells (54, 68). The upstream regulator analysis also implicated IFNG (activation Z-score=6.1).

339

340 Because these regulators were not detected by RNAseq, presumably due to insufficient sequencing
341 depth, we used qPCR to measure decidual expression of *Il12p35*, *Ebi3* and *Il10*, as well as *Tgfb1*,
342 another key Treg cell-derived immune regulatory cytokine (67), plus uNK cell factors *Ifng* and

343 *Vegf* involved in vascular remodelling (35, 37, 51). In the same GD10.5 decidual samples utilised
344 in the RNA sequencing analysis, peri-implantation Treg cell depletion resulted in a 62% reduction
345 in *Ebi3* expression and a 58% downregulation of *Il12p35* expression, compared to control
346 *Foxp3^{DTR}* mice (Figure 9A-B). Similarly, *Il10* was reduced by 48% and *Tgfb1* was reduced by
347 60% after Treg cell depletion (Figure 9C, D). In contrast decidual *Ifng* was not impacted (Figure
348 9E), but *Vegfa* expression was reduced by 57% compared to control mice (Figure 9H). Decidual
349 expression of *Foxp3* mRNA encoding the Treg cell transcription factor FOXP3 was reduced by
350 71% after earlier Treg cell depletion (Figure 9G), while *Ncr1* encoding the uNK cell maturation
351 marker NKp46 was reduced by 60% (Figure 9F), consistent with the histological finding of fewer
352 uNK cells in decidual tissues.

353

354 **DISCUSSION**

355 There is compelling evidence that dysregulation in the number or function of Treg cells contributes
356 to the pathophysiological origin of preeclampsia and related pregnancy complications (69, 70) but
357 whether and how Treg cells contribute to the uterine and placental dysfunction underpinning these
358 conditions remains unclear. In this study, *Foxp3^{DTR}* mice were used to selectively and transiently
359 deplete Treg cells to investigate their role in the critical process of decidual spiral artery
360 remodeling required in early pregnancy for robust placental development and function. Here, we
361 demonstrate that Treg cell depletion causes impaired spiral artery remodeling, resulting in fetal
362 loss and fetal growth restriction. Treg cell depletion was associated with an altered transcriptional
363 profile in the decidua that along with histochemical analysis implicates dysregulation of uNK cells
364 and extravillous trophoblasts in mid-gestation. In particular, depletion of Treg cells caused
365 upregulation of genes involved in NK cell interferon signaling and cytotoxic function, notably

366 granzyme-mediated programmed cell death signalling. Treg cell replacement experiments largely
367 rescued the reproductive phenotype and reversed the gene expression changes, confirming that
368 Treg cells affect decidual spiral artery remodeling, and supporting the inference of a mechanism
369 involving Treg cell modulation of uNK cell functional status. This requirement for Treg cells
370 provides new insight into immune regulation of uterine vascular remodeling, extending our
371 previous demonstration of a role for Treg cells in regulating the main uterine arteries in pregnancy
372 (19). If a similar effect of Treg cells on uterine vascular remodelling occurs in women, Treg cell
373 deficiency would act to constrain the placental vascular supply, contributing to development of
374 preeclampsia and other pregnancy disorders characterized by impaired placentation including
375 recurrent miscarriage, fetal growth restriction and spontaneous preterm birth (2).

376

377 After embryo implantation in mice the uterine lining undergoes decidualization and extravillous
378 trophoblasts invade the decidua both interstitially and endovascularly, to progress remodeling of
379 the decidual spiral arteries and enable placental growth (71, 72) and full access to the maternal
380 blood supply by GD10.5 (30, 47). Remodeling is a process that involves displacement of
381 endothelial cells and smooth muscle cells from the spiral artery wall, converting them to flaccid
382 conduits. uNK cells are the main maternal immune cells present in the decidua at the time of
383 implantation (34, 41). They engage with trophoblasts in clusters around spiral arteries and are
384 paramount in facilitating the remodeling process through secreting cytokines and proteases (37,
385 39). Treg cells, macrophages, and other immune cells are positioned within the decidual stroma
386 with the potential to interact with uNK cells, as well as trophoblast cells, decidual cells, spiral
387 artery smooth muscle cells, and endothelial cells (2, 32). There is evidence of cross-regulation
388 between these immune cells, such that together they ensure correct uNK cell function (73, 74).

389

390 Our experiments imply that a primary cause of pregnancy loss in late gestation following Treg cell
391 depletion in early pregnancy is placental insufficiency due to inadequate remodeling of decidual
392 spiral arteries in early pregnancy. Spiral arteries from Treg cell-depleted mice had a smaller lumen
393 and cross-sectional area, and failed to exhibit the expected loss of smooth muscle actin. This was
394 accompanied by a trend towards increased relative wall thickness when Treg cells were depleted.
395 Importantly, all of these markers of spiral artery remodeling were normalized when mice were pre-
396 treated with wild-type Treg cells to prevent Treg cell deficiency.

397

398 A combination of immunohistochemical and RNAseq data point to a role for Treg cells in
399 modulating uNK cells. uNK cell subsets can be distinguished by their reactivity to DBA lectin,
400 which detects GalNAc (75), a glycosylated structure acquired during functional maturation after
401 conception (51, 52). DBA⁺ uNK cells are more abundant than DBA⁻ uNK cells in the decidua and
402 exhibit pro-angiogenic activity. Treg cell depletion reduced DBA⁺ uNK cells in the decidua, and
403 this was mitigated by Treg cell replacement. DBA⁺ uNK cells express higher levels of *Vegfa*, *Il22*,
404 and *Pgf* compared to DBA⁻ uNK cells, consistent with a contribution to decidual angiogenesis,
405 while DBA⁻ uNK cells express more *Ifng*, which also plays a role in remodeling of the decidual
406 vasculature (35, 51).

407

408 We analyzed uNK cells utilizing a flow cytometry panel designed to detect trNK cells, cNK cells
409 and ILC1 cells, without regard to their DBA expression. trNK cells are resident within the decidua
410 and express angiogenic factors, cNK cells are recruited from peripheral blood and are similar to
411 splenic NKs, while ILC1s arise from trNK cells residing in the non-pregnant uterus (76) but do

412 not express the NK cell-specific transcription factor, EOMES (58, 77). Flow cytometry did not
413 reveal any change in the relative proportion of the three uNK subsets in Treg cell deficient mice.
414 We therefore undertook RNAseq to assess the impact of Treg cell depletion on decidual gene
415 expression. We demonstrate that when Treg cells are depleted, transcriptional changes indicating
416 inappropriate NK cell and T cell activation arise, and mostly these were restored to varying degrees
417 by Treg cell pre-treatment.

418

419 Amongst the genes most strongly induced after Treg cell depletion were granzyme serine proteases
420 that mediate NK cell and T cell-mediated cytotoxicity. Granzymes can exert non-cytotoxic
421 enzymatic actions that cause tissue damage, remodel extracellular matrices, and induce pro-
422 inflammatory cytokine release, so a range of consequences of elevated granzymes might contribute
423 to the decidual changes seen after Treg cell depletion. While it is not possible from the data
424 presented here to conclusively define the relative contribution of uNK cells versus T cells to these
425 changes, for several reasons we consider that uNK cells are centrally involved. Previous studies
426 show that T cells are a minor component of the decidual leukocyte population, whereas NK cells
427 predominate. That Treg cell depletion caused the prominent NK gene *Prf1* (encoding the pore-
428 forming protein perforin-1) and NK cell transcription factors *Eomes*, *Id2* and *Runx3* to be induced
429 suggests an altered uNK cell transcriptional program. Our analysis did not indicate expansion of
430 effector CD3⁺ or CD4⁺ T cells after Treg cell depletion. The decidua has specific mechanisms to
431 exclude effector T cells by epigenetic silencing of chemokine genes *Cxcl9*, *Cxcl10*, and *Ccl5* (78),
432 and no change in expression of these genes was seen after Treg cell depletion. Collectively these
433 data imply that uNK cells contribute to the altered decidual gene expression and the mechanisms
434 underpinning impaired vascular remodelling. Further analysis will be needed to definitively

435 understand how uNK cell functions are affected by Treg cells and how in turn this leads to altered
436 vascular remodelling. It will also be important to evaluate whether specific effector T cell subsets
437 such as CD8⁺ T cells and gamma delta T cells, that can express granzymes and potentially elicit
438 fetal loss (79, 80), might also contribute to the decidual changes we observed after Treg cell
439 depletion.

440

441 The RNAseq data also point to altered decidual trophoblast invasion after Treg cell depletion.
442 Several trophoblast genes were upregulated, including several associated with placental glycogen
443 cells, while genes expressed by other extravillous trophoblast lineages were downregulated. This
444 result is consistent with the histological data showing elevated abundance of glycogen cells, a
445 specific subset of trophoblasts that store glycogen to serve late gestation fetal growth in the phase
446 just prior to parturition (81). Although there were no apparent effects of Treg cell depletion on
447 placental weight in late-gestation, the reduced fetal:placental weight ratio implies impaired
448 placental efficiency. In several mouse models of complicated pregnancy, placental glycogen is not
449 mobilized and instead is retained in the junctional zone (82-84). Retained placental glycogen has
450 also been implicated in humans with preeclampsia and gestational diabetes (84).

451

452 There is extensive evidence of cross-talk between uNK and trophoblasts in the decidua.
453 Trophoblasts influence the maturation of uNK precursor cells into mature uNK and uNK both
454 promote and constrain EVT migration and invasion of spiral arteries (85, 86). The reduced
455 expression of trophoblast genes might imply excessive uNK cell constraint of trophoblast invasion
456 after peri-implantation Treg cell depletion, but whether uNK cell cytotoxicity is involved will
457 require further analysis. Although uNK express granzymes and perforin-1 even under normal

458 circumstances, uNK cells do not exhibit killing of trophoblasts or fetal cells in the manner of
459 peripheral blood NK cells (87), except under very specific circumstances, for example in the event
460 of viral (88) or bacterial infection (89). Given that in the current study, placental integrity was not
461 overtly changed after Treg cell depletion, we consider uNK cell cytotoxic activity to be unlikely
462 and instead, non-cytotoxic effects of uNK granzymes on trophoblast invasion and the decidual
463 vasculature warrant investigation. Single-cell sequencing experiments will be informative in this
464 regard.

465

466 Decidual gene expression analysis by qPCR revealed a potential role for cytokines TGF β , IL35,
467 and IL10 in communication between Treg cells and uNK cells. IL35 is produced almost
468 exclusively by Treg cells (90, 91) and has an established role in suppressing effector functions (92,
469 93), including in NK cells (68). IL10 is an anti-inflammatory cytokine produced by both immune
470 and non-immune cells including Treg cells, uNK cells, macrophages, and trophoblast cells (94). It
471 is well established that IL10 is critical for immune tolerance in pregnancy (95), and IL10 null
472 mutant mice exhibit elevated NK1.1⁺ decidual cell numbers and cytotoxic capacity (96). TGF β
473 can induce NK cell proliferation, upregulate NKp46 expression (97), and promote a more
474 tolerogenic phenotype in NK cells (98). Reduced expression in each of these cytokines after Treg
475 cell depletion presumably reflects their synthesis in Treg cells, particularly for IL35 which is
476 restricted to this cell lineage. Treg cell release of TGF β , IL10 and IL35 are implicated in Treg cell-
477 mediated protection of the vasculature in other tissues (99-103). Treg cells constrain vascular
478 inflammation in atherosclerosis (20, 21), but Treg cell-NK cell communication affects vascular
479 biology in other tissues is unknown. Such an interaction is possible given evidence of NK cell-
480 Treg cell interactions in a range of settings (104-106).

481

482 Decidual gene expression analysis also revealed that *Vegfa* transcription was reduced in Treg cell-
483 depleted mice. Given evidence that production of VEGFA by DBA⁺ uNK cells is important for
484 angiogenesis and remodeling of the decidual vasculature (39), this finding is consistent with our
485 histochemical data showing decreased DBA⁺ uNK cells. Our finding that IFN γ remained
486 unchanged after Treg depletion is consistent with Treg cells exerting a greater effect on DBA⁺
487 uNK cells producing VEGF, than DBA⁻ uNK cells secreting IFN γ (39).

488

489 As well as decidual spiral artery remodeling, Treg cells are implicated in modifying the systemic
490 vasculature and notably the uterine artery. After Treg cell depletion, we saw increased resistance
491 to blood flow in the main uterine arteries in mid-gestation, and this was prevented with Treg cell
492 replacement, confirming our earlier findings. Together with observations that Treg cell deficiency
493 promotes generation of the vasoconstrictor endothelin-1 in uterine arteries (19), this demonstrates
494 that Treg cells are necessary for normal function of the uterine artery in mid-gestation, as well as
495 late gestation (17). The effects of Treg cell depletion on the systemic vasculature may be limited
496 to the window during which Treg cells are deficient, as we found that uterine artery resistance was
497 normalized after Treg cell populations recovered.

498

499 Collectively our data on structural indicators of placental transport efficiency and compromised
500 fetal growth in late pregnancy indicate a pathological state that is the consequence of early
501 gestation immune perturbation. This sequence of events is reminiscent of other pro-inflammatory
502 perturbations in early pregnancy that manifest as impaired vascular remodeling, altered placental
503 development, followed by fetal loss and or growth restriction in late gestation (30). That all the

504 vascular defects, as well as fetal loss, could be rescued by transfer of wild-type Treg cells alleviates
505 concern of off-target effects of DT, and confirms that the consequences of DT treatment can be
506 attributed to Treg cells. Although Treg cell replacement did not improve fetal weight, it did
507 improve parameters of fetal growth including crown-to-rump length, abdominal girth, and
508 biparietal diameter, and independent experiments in C57Bl/6 showed no adverse impact on fetal
509 growth of DT administration. This implies that the fetal weight deficit remaining after Treg
510 replacement is due to incomplete recapitulation of the unperturbed immune state, as opposed to
511 deleterious effects of DT. While these data clearly show an impact of Treg cells on the decidual
512 vasculature and implicate a mediating role for uNK cells, we do not exclude the possibility that
513 other effects of Treg cell depletion, mediated locally in the implantation site or systemically in
514 other tissues, also contribute to fetal loss and growth restriction.

515

516 Impaired vascular remodeling of the maternal spiral arteries is the pathological antecedent of
517 preeclampsia (13), resulting in poor uteroplacental perfusion later in pregnancy and often leading
518 to fetal growth restriction. A possible role of Treg cells in facilitating the spiral artery remodeling
519 process has been speculated, but definitive evidence has been lacking (2, 107). Aberrations in uNK
520 cells have been investigated as a possible contributing factor to impaired spiral artery remodeling
521 in preeclampsia. There are conflicting reports on altered uNK cell numbers in preeclampsia (108-
522 111), indicating the need for further research to resolve these conflicting observations.

523

524 In conclusion, this study provides new evidence demonstrating that Treg cells are essential for
525 remodeling of decidual spiral arteries in early pregnancy and identifies a candidate mechanism
526 involving Treg cell regulation of uNK cells (Figure 10). Given the consistent finding of

527 perturbed Treg cells in preeclampsia and related hypertensive pregnancy complications, these
528 findings indicate that studies to determine effects of Treg cells on spiral artery remodeling in
529 women are warranted and add to the imperative to consider Treg cells as a potential therapeutic
530 target in at-risk women.

531

532 **METHODS**

533 **Sex as a biological variable**

534 Our study focused on pregnancy and therefore outcomes were focused on female mice. Male mice
535 were used for mating purposes. Ongoing investigations are examining potential impacts on both
536 male and female offspring.

537

538 **Animals**

539 *Foxp3*^{DTR} (Forkhead box P3-diphtheria toxin receptor; B6.129(Cg)-*Foxp3*^{tm3(DTR/GFP)Ayr/J}) mice
540 were purchased from Jackson Laboratories (Bar Harbour, Maine USA), and C57Bl/6 (WT) female
541 and BALB/c male mice were purchased from Animal Resources Centre (Western Australia,
542 Australia). Mice were housed and bred in a specific pathogen-free facility. Female mice (8-12
543 weeks) were housed with proven fertile males, and the presence of a copulatory plug was
544 designated gestational day (GD)0.5. See Supplemental Methods for details.

545

546 **Treg cell depletion**

547 To induce Treg cell depletion, *Foxp3*^{DTR} mice were injected with DT from *Corynebacterium*
548 *diphtheria* (Sigma-Aldrich) (37.5 ng/g, i.p) on GD 3.5 and 5.5. Vehicle (PBS)-treated *Foxp3*^{DTR}
549 mice were controls in all experiments. See Supplemental Methods for details.

550

551 **T cell isolation and adoptive transfer**

552 CD4⁺CD25⁺ Treg cells or CD4⁺CD25⁻ Tconv cells were isolated from the uterine-draining, para-
553 aortic lymph nodes (uDLN), and the mesenteric, inguinal, and brachial lymph nodes and spleen

554 from pregnant wild-type C57BL/6 mice at GD10.5 to 13.5. Cells were adoptively transferred by
555 i.v. injection into DT-treated *Foxp3^{DTR}* on GD3.5 and 5.5. See Supplemental Methods for details.

556

557 **Flow cytometry**

558 On GD6.5 and GD10.5, single-cell suspensions were prepared from uDLN, mesenteric LN and
559 pooled decidua from *Foxp3^{DTR}* mice. Cells were stained using fluorophore-conjugated antibodies
560 to detect surface and intracellular markers (Supplemental Table 5) and a standardized gating
561 strategy (Supplemental Figure 11 and 12). See Supplemental Methods for details.

562

563 **Ultrasound biomicroscopy**

564 Uterine artery function was assessed on GD9.5 and uterine and umbilical artery function assessed
565 at GD17.5, using an MX550D transducer probe on an ultrasound biomicroscope (model Vevo
566 2100, VisualSonics®, ON, Canada) in *Foxp3^{DTR}* mice. See Supplemental Methods for details.

567

568 **Histology, immunohistochemistry and lectin staining**

569 Mid-sagittal sections from formalin-fixed, paraffin-embedded GD10.5 implantation sites (for
570 decidual spiral artery analysis; Supplemental Figure 13) and GD18.5 placentas were stained with
571 Masson's trichrome. Smooth muscle cells were detected with α -SMA and uNK cells with
572 biotinylated DBA-lectin. See Supplemental Methods for details.

573

574 **RNA sequencing, and data analysis**

575 RNA from decidual tissues were extracted as described previously (12). Library preparation and
576 sequencing on NovaSeq X at 80 million reads per sample was performed by the South Australian

577 Genomics Centre. Sequencing reads were mapped to GRCm38 (mm10) mouse genome and
578 quantified using STAR (112). Limma-voom (113) was then used on TMM normalized reads to
579 identify genes that were differentially expressed (DEGs, FDR <0.1) according to treatment group.
580 Overrepresentation pathway analysis was performed with *clusterProfiler* (114). The Mouse
581 Genomics Informatics resource (65) and mouse placenta single cell sequencing data (66) was used
582 to identify genes enriched in placental trophoblasts. See Supplemental Methods for details and
583 data availability.

584

585 **Statistics**

586 Data were analysed by unpaired t-test or Mann-Whitney U test, or one-way ANOVA or Kruskal-
587 Wallis test, depending on normality of data distribution. Fetal outcome data were analysed by
588 mixed model ANOVA analysis with mother as subject and litter size as covariate. Analysis was
589 performed using GraphPad Prism, SPSS, or R in the case of RNA sequencing data. See
590 Supplemental Methods for details.

591

592 **Study Approval**

593 All experiments were approved by the University of Adelaide Animal Ethics Committee, ethics
594 numbers M-2018-127, M-2017-024 and M-2020-107 in accordance with the Australian Code of
595 Practice for the Care and Use of Animals for Scientific Purposes (8th edition, 2013). See
596 Supplemental Methods for details.

597

598 **Data availability**

599 Values for all data points in graphs are reported in the Supporting Data Values XLS files. Complete
600 R code used to analyze and visualize the RNA-sequencing data have been deposited at
601 https://tranmanhha135.github.io/Treg_uNK/. Raw fastq files have been deposited in the National
602 Center for Biotechnology Information's Gene Expression Omnibus database (GSE267364).
603

604 **AUTHOR CONTRIBUTIONS**

605 ASC and SAR designed the studies. SLH, HMG, HYC, HMT, LMM, EAKL and ASC conducted
606 experiments and analysed data. SLH, ASC, HMT and LMM prepared figures. KLF, CTR, and
607 STD provided specific expertise and made substantial contributions to designing experiments and
608 interpreting data. ASC and SAR wrote the manuscript. All authors revised drafts and reviewed the
609 manuscript.

610

611 **ACKNOWLEDGEMENTS**

612 ASC was supported by a Future Leader Fellowship (101998) of the National Heart Foundation of
613 Australia and an Early Career Fellowship (GNT1092191) from the National Health and Medical
614 Research Council (NHMRC) of Australia. This study was supported by funding to ASC from the
615 NHMRC Ideas Grant (GNT2002129), the Channel 7 Children's Research Foundation (181563),
616 the Ian Potter Foundation (project 20190089). SAR was supported by NHMRC Investigator
617 Grant APP1198172. SLH was supported by the Westpac trust foundation and an Australian
618 Government funded Research Training Program Stipend (RTPS). CTR was supported by a
619 NHMRC Investigator Grant (GNT1174971) and a Matthew Flinders Fellowship from Flinders
620 University. We would like to acknowledge the support of Adelaide Microscopy and Microscopy
621 Australia (ROR: 042mm0k03) in the Faculty of Health and Medical Sciences, the University of
622 Adelaide, enabled by NCRIS.

623

624 **FIGURE LEGENDS**

625

626 **Figure 1: Effect of DT administration to *Foxp3*^{DTR} mice in the peri-implantation period on**
627 **uterine draining, para-aortic lymph node (uDLN) Treg cell proportion and phenotype in**
628 **mid-gestation.** *Foxp3*^{DTR} mice were administered PBS (veh) or DT i.p. on GD3.5 and GD5.5.
629 uDLN were recovered on GD6.5 or GD10.5 and the proportion and phenotype of CD4⁺FOXP3⁺
630 Treg cells were evaluated using flow cytometry. (A) Representative contour plots show the
631 proportion of CD4⁺FOXP3⁺ Treg cells in the uDLN on GD6.5 from vehicle-treated (left) and DT-
632 treated (right) *Foxp3*^{DTR} mice. (B) The proportion of CD4⁺FOXP3⁺ Treg cells in uDLN at GD6.5
633 and GD10.5. Detailed analysis of Treg cells at GD10.5 shows the proportion of Treg cells
634 expressing NRP1 indicating thymic origin (C), proliferation marker Ki67 (D), and marker of
635 suppressive competence CTLA4 (E). The proportion of IFN γ ⁺CD4⁺FOXP3⁻ (Th1 cells; F) and
636 IL17a⁺CD4⁺FOXP3⁻ (Th17 cells; G) were measured.. N=3-14 mice per group. Data are
637 mean \pm SEM. Data points are values from individual dams. Analysis was by two-tailed t-test or
638 Mann Whitney U test depending on normality of data distribution for data in (C-G). Data in (B)
639 were analysed using a 1-way ANOVA comparing samples within the same gestational day.
640 *P<0.05; **P<0.01; ***P<0.001.

641

642 **Figure 2: Treg cell depletion in the peri-implantation period results in reduced litter size at**
643 **birth and increased fetal loss in late gestation and is mitigated by Treg cell transfer.** *Foxp3*^{DTR}
644 mice were administered PBS (veh) or DT i.p. on GD3.5 and GD5.5, then pregnancy outcomes
645 were assessed either at birth (B-F), or on GD18.5 (G-J). Some mice also received wild-type Treg
646 cells or Tconv cells on GD2.5 and GD4.5. (A) Schematic diagram showing the treatment and

647 analysis protocol (created with BioRender.com). **(B)** Proportion of mated mice that delivered at
648 least one viable pup at birth. **(C)** Total number of pups at birth per dam. **(D)** Number of viable
649 pups within 24 h of birth per dam. **(E)** proportion of viable pups within 24 h of birth per dam. **(F)**
650 Pup weight at 24-36 h after birth. **(G)** The proportion of dams carrying a viable pregnancy at
651 GD18.5 (defined as at least one viable implantation site). **(H)** Number of total fetuses per dam at
652 GD18.5. **(I)** Number of viable fetuses per dam at GD18.5. **(J)** Number, and **(K)** proportion of
653 resorbing fetuses per dam at GD18.5. Numbers of mice **(B)** and dams **(G)** in each group are shown
654 in parentheses. Data are mean±SEM. Data points are values from individual dams. Analysis was
655 by chi-squared test **(B and G)** or one-way ANOVA with two-tailed posthoc t-test **(C-F, H-K)**.
656 *P<0.05; **P<0.01; ***P<0.001.

657

658

659 **Figure 3: Treg cell depletion in the peri-implantation period causes fetal growth restriction**
660 **that is mitigated by Treg cell transfer.** *Foxp3^{DTR}* mice were administered PBS (veh) or DT i.p.
661 on GD3.5 and GD5.5, then fetal and placental development were assessed on GD18.5. Some mice
662 also received wild-type Treg cells or Tconv cells on GD2.5 and GD4.5. **(A)** Representative images
663 of fetuses, **(B)** fetal weight, **(C)** placental weight, and **(D)** fetal to placental weight ratio. The
664 distribution of **(E)** fetal weights, **(F)** placental weights, and **(G)** fetal to placental weight ratio were
665 calculated. **(H)** Fetal crown-to-rump length, **(I)** abdominal girth, and **(J)** biparietal diameter.
666 Vertical dashed line represents the 10th centile of the curve (1.15 g, 0.08 g and 11.45 in E, F and
667 G, respectively). N= 2-11 fetuses from 14-19 dams per group. Fetal and placental data are shown
668 as violin plots with median and quartile values marked. Analysis was by mixed model ANOVA

669 with mother as subject and litter size as covariate. *P<0.05; **P<0.01; ***P<0.001. Scale bar = 1
670 cm.

671

672 **Figure 4: Treg cell depletion impairs spiral artery remodeling in mid-gestation.** Pregnant
673 *Foxp3^{DTR}* were administered PBS (veh) or DT i.p. on GD3.5 and GD5.5, then tissues were
674 collected on GD10.5. Some mice also received wild-type Treg cells or Tconv cells on GD2.5 and
675 GD4.5, then tissues were collected on GD10.5. Representative images of mid-sagittal sections of
676 uterus stained with Masson's trichrome (**A-D**), or to detect α -smooth muscle actin (**E-H**). Black
677 arrowheads indicate spiral arteries, black arrows indicate α -smooth muscle actin-positive cells.
678 Parameters including (**I**) average lumen area of spiral arteries, (**J**) lumen diameter, (**K**) the vessel
679 to lumen area ratio, and (**L**) proportion of decidual cells positive for α -smooth muscle actin, are
680 shown. N=2 implantation sites per dam from 8-12 dams per group. Data are mean \pm SEM. Data
681 points are average values for individual dams. Analysis was by one-way ANOVA with two-tailed
682 posthoc t-test. *P<0.05; **P<0.01; ****P<0.0001. Scale bars; A-D = 1 mm; insets = 50 μ m;
683 = 50 μ m.

684

685 **Figure 5: Uterine artery resistance in mid-gestation is increased by Treg cell depletion and**
686 **mitigated by Treg cell replacement.** Pregnant *Foxp3^{DTR}* mice were administered PBS (veh) or
687 DT i.p. on GD3.5 and GD5.5, then tissues were collected on GD10.5. Some mice also received
688 wild-type Treg cells or Tconv cells on GD2.5 and GD4.5. Measurements were taken on GD9.5.
689 (**A**) Representative waveforms of uterine arteries. (**B**) Resistance index and (**C**) pulsatility index
690 were calculated. N=5-8 dams per group. Data are mean \pm SEM. Data points are average values for
691 individual dams. Analysis was by one-way ANOVA with two-tailed posthoc t-test. EDV indicates

692 end-diastolic velocity; PSV, peak systolic velocity and TAV, time-averaged velocity. *P<0.05;
693 **P<0.01.

694

695 **Figure 6: Treg cell depletion causes a reduction in DBA⁺ uNK cells in mid-gestation that is**
696 **mitigated by Treg cell transfer.** Pregnant *Foxp3^{DTR}* mice were administered PBS (veh) or DT
697 i.p. on GD3.5 and GD5.5, then tissues were collected on GD10.5. Some mice also received wild-
698 type Treg cells or Tconv cells on GD2.5 and GD4.5. Tissues were collected on GD10.5. (A-D)
699 Decidual tissue sections were labelled with biotinylated *Dolichos biflorus* agglutinin (DBA)-lectin
700 to detect the DBA⁺ subset of uNK cells that predominates in pregnancy (brown stain, arrows). (E)
701 The percent positivity for DBA⁺ uNK cells was quantified. (F) The decidual region of each section
702 (marked, dotted line in A) was identified and measured. N=2 implantation sites per dam, 8-12
703 dams per group. Data are mean±SEM. Data points are average values for individual dams.
704 Analysis was by one-way ANOVA with two-tailed posthoc t-test. ****P<0.0001. Scale bars:
705 outset = 500 µm; insets = 100 µm.

706

707 **Figure 7: Treg cell depletion causes a perturbation in decidual transcription profile in**
708 **midgestation that is mitigated by Treg cell transfer.** Pregnant *Foxp3^{DTR}* mice were administered
709 PBS (veh; n=6) or DT (n=5) i.p. on GD3.5 and GD5.5, and decidual tissue was collected on
710 GD10.5. Some mice (n=5) also received wild-type Treg cells on GD2.5 and GD4.5. (A) Principle
711 component analysis (PCA) of filtered genes, illustrating gene expression patterns in individual
712 samples. (B) The number of DEGs (FDR<0.1) that overlap between DT-treated mice compared to
713 PBS vehicle control (purple) and DT+Treg-treated mice compared to DT-treated mice (green).
714 (C) Functional heatmap of DEGs (FDR<0.1) and their relationship to enriched terms/pathways

715 identified using Gene Ontology (GO, FDR < 0.05), Kyoto Encyclopedia of Genes and Genomes
716 (KEGG, FDR<0.2), Reactome (FDR < 0.1), and Ingenuity Pathway Analysis (IPA, P<0.05)
717 databases.

718

719 **Figure 8: Treg cell depletion causes a perturbation in decidual trophoblast genes in**
720 **midgestation that is mitigated by Treg cell transfer.** Pregnant *Foxp3*^{DTR} mice were
721 administered PBS (veh; n=6) or DT (n=5) i.p. on GD3.5 and GD5.5, and decidual tissue was
722 collected on GD10.5. Some mice (n=5) also received wild-type Treg cells on GD2.5 and GD4.5.
723 Functional heatmap of DEGs (FDR <0.1) identified as indicative of altered extravillous
724 trophoblasts on the basis of both: (1) reported expression in specific mouse trophoblast cell types
725 (colour coded, LHS) (extracted from published single cell RNA-seq data (66)); and (2) expression
726 in mouse placenta but not mouse uterus, according to Mouse Genomics Informatics database (see
727 Materials and Methods for details). Cell labels indicate the FDR-adjusted *P* value (FDR) of DEGs
728 present in the RNA-seq dataset. *FDR <0.1; **FDR <0.05; FDR <0.01. 1' P-TGC, primary
729 parietal trophoblast giant cell; 2' P-TGC, secondary parietal trophoblast giant cells; EPC,
730 ectoplacental cone; Gly-T, glycogen trophoblast cells; LaTP, labyrinthine trophoblast; S-TGC,
731 sinusoid trophoblast giant cell; Spa-TGC, spiral artery-associated trophoblast giant cell; SpT,
732 spongiotrophoblast cell; SynT1, multinucleated syncytiotrophoblast cells; TSC, trophoblast stem
733 cell; ExE, extraembryonic ectoderm.

734

735 **Figure 9: Peri-implantation Treg depletion elicits reduction of anti-inflammatory**
736 **decidual gene transcripts.** Pregnant *Foxp3*^{DTR} mice were given PBS (veh) or DT on GD3.5 and
737 GD5.5, then tissues were collected on GD10.5. (A) *Ebi3* and (B) *Il12p35* genes encoding IL35,
738 (C) *Il10*, (D) *Tgfb1*, (E) *Ncr1* encoding NKp46, (F) *Foxp3* encoding FOXP3 transcription factor

739 necessary for Treg cell development, and (G) *Vegfa*, were quantified by qPCR. N=9-10 dams per
740 group. Data are presented as mean±SEM. Each data point represents the average of two decidua
741 per dam. Analysis was by unpaired t-test. *P<0.05; **P<0.01; ***P<0.001.

742 Pregnant *Foxp3*^{DTR} mice were given PBS (veh) or DT on GD3.5 and GD5.5, then tissues were
743 collected on GD10.5. (A) *Ebi3* and (B) *Il12p35* genes encoding IL35, (C) *Il10*, (D) *Tgfb1*, (E)
744 *Ncr1* encoding NKp46, (F) *Foxp3* encoding FOXP3 transcription factor necessary for Treg cell
745 development, and (G) *Vegfa*, were quantified by qPCR. N=9-10 dams per group. Data are
746 mean±SEM. Each data point represents the average of two decidua per dam. Analysis was by
747 unpaired t-test. *P<0.05; **P<0.01; ***P<0.001.

748

749 **Figure 10: Schematic illustration of current working hypothesis on mechanisms of Treg cell-**
750 **mediated regulation of decidual spiral artery remodeling.** Treg cells modulate the decidual
751 microenvironment to facilitate decidual spiral artery remodelling in early pregnancy in mice. When
752 Treg cells are deficient, spiral artery remodeling is impaired. In turn this causes fetal growth
753 restriction and late gestation fetal loss that is exacerbated by increased resistance to blood flow in
754 the uterine arteries. Treg cell support of spiral artery remodelling is likely to be mediated through
755 Treg cell effects in a decidual network involving uNK cells and trophoblasts. Our data show
756 reduced numbers of DBA⁺ uNK cells, and plus attenuation of genes associated with uNK cell
757 function and extravillous trophoblast invasion. Since uNK cells are known to be essential for spiral
758 artery remodelling through IFN γ and VEGF production, and Treg cells produce cytokines TGF β ,
759 IL10, and IL35 known to regulate uNK cell function, a direct effect of Treg cells on uNK cells is
760 implicated. Altered extravillous trophoblast invasion and/or survival in the decidua may also be

761 involved, since extravillous trophoblasts interact with uNK cells and contribute to spiral artery

762 remodelling. See text for details. Created with BioRender.com.

763

764 **REFERENCES**

- 765
- 766 1. Vignali DAA, Collison LW, and Workman CJ. How regulatory T cells work. *Nature*
767 *Reviews Immunology*. 2008;8(7):523-32.
- 768 2. Robertson SA, Care AS, and Moldenhauer LM. Regulatory T cells in embryo implantation
769 and the immune response to pregnancy. *The Journal of Clinical Investigation*.
770 2018;128(10):4224-35.
- 771 3. Erlebacher A. Mechanisms of T cell tolerance towards the allogeneic fetus. *Nature Reviews*
772 *Immunology*. 2013;13(1):23-33.
- 773 4. Aluvihare VR, Kallikourdis M, and Betz AG. Regulatory T cells mediate maternal
774 tolerance to the fetus. *Nature immunology*. 2004;5(3):266-71.
- 775 5. Shima T, Sasaki Y, Itoh M, Nakashima A, Ishii N, Sugamura K, and Saito S. Regulatory
776 T cells are necessary for implantation and maintenance of early pregnancy but not late
777 pregnancy in allogeneic mice. *Journal of reproductive immunology*. 2010;85(2):121-9.
- 778 6. Teles A, Schumacher A, Kuhnle MC, Linzke N, Thuere C, Reichardt P, et al. Control of
779 uterine microenvironment by foxp3(+) cells facilitates embryo implantation. *Front*
780 *Immunol*. 2013;4:158.
- 781 7. Sasaki Y, Darmochwal-Kolarz D, Suzuki D, Sakai M, Ito M, Shima T, et al. Proportion of
782 peripheral blood and decidual CD4(+) CD25(bright) regulatory T cells in pre-eclampsia.
783 *Clin Exp Immunol*. 2007;149(1):139-45.
- 784 8. Quinn KH, Lacoursiere DY, Cui L, Bui J, and Parast MM. The unique pathophysiology of
785 early-onset severe preeclampsia: role of decidual T regulatory cells. *Journal of*
786 *Reproductive Immunology*. 2011;91(1):76-82.
- 787 9. Prins JR, Boelens HM, Heimweg J, Van der Heide S, Dubois AE, Van Oosterhout AJ, and
788 Erwich JJ. Preeclampsia is associated with lower percentages of regulatory T cells in
789 maternal blood. *Hypertens Pregnancy*. 2009;28(3):300-11.
- 790 10. Darmochwal-Kolarz D, Kludka-Sternik M, Tabarkiewicz J, Kolarz B, Rolinski J,
791 Leszczynska-Gorzela B, and Oleszczuk J. The predominance of Th17 lymphocytes and
792 decreased number and function of Treg cells in preeclampsia. *J Reprod Immunol*.
793 2012;93(2):75-81.
- 794 11. Steinborn A, Haensch GM, Mahnke K, Schmitt E, Toermer A, Meuer S, and Sohn C.
795 Distinct subsets of regulatory T cells during pregnancy: is the imbalance of these subsets
796 involved in the pathogenesis of preeclampsia? *Clin Immunol*. 2008;129(3):401-12.
- 797 12. Duley L. The global impact of pre-eclampsia and eclampsia. *Semin Perinatol*.
798 2009;33(3):130-7.
- 799 13. Steegers EA, von Dadelszen P, Duvekot JJ, and Pijnenborg R. Pre-eclampsia. *Lancet*.
800 2010;376(9741):631-44.
- 801 14. Santner-Nanan B, Peek MJ, Khanam R, Richarts L, Zhu E, Fazekas de St Groth B, and
802 Nanan R. Systemic increase in the ratio between Foxp3+ and IL-17-producing CD4+ T
803 cells in healthy pregnancy but not in preeclampsia. *J Immunol*. 2009;183(11):7023-30.
- 804 15. Robertson SA, Bromfield JJ, and Tremellen KP. Seminal 'priming' for protection from pre-
805 eclampsia-a unifying hypothesis. *J Reprod Immunol*. 2003;59(2):253-65.
- 806 16. Green ES, Moldenhauer LM, Groome HM, Sharkey DJ, Chin PY, Care AS, et al.
807 Regulatory T cells are paramount effectors in progesterone regulation of embryo
808 implantation and fetal growth. *JCI Insight*. 2023;8(11).

- 809 17. Cornelius DC, Amaral LM, Harmon A, Wallace K, Thomas AJ, Campbell N, et al. An
810 increased population of regulatory T cells improves the pathophysiology of placental
811 ischemia in a rat model of preeclampsia. *American Journal of Physiology - Regulatory,*
812 *Integrative and Comparative Physiology.* 2015;309(8):R884.
- 813 18. Saftlas AF, Rubenstein L, Prater K, Harland KK, Field E, and Triche EW. Cumulative
814 exposure to paternal seminal fluid prior to conception and subsequent risk of preeclampsia.
815 *J Reprod Immunol.* 2014;101-102:104-10.
- 816 19. Care AS, Bourque SL, Morton JS, Hjartarson EP, Robertson SA, and Davidge ST.
817 Reduction in Regulatory T Cells in Early Pregnancy Causes Uterine Artery Dysfunction in
818 Mice. *Hypertension.* 2018;72(1):177-87.
- 819 20. Spitz C, Winkels H, Bürger C, Weber C, Lutgens E, Hansson GK, and Gerdes N.
820 Regulatory T cells in atherosclerosis: critical immune regulatory function and therapeutic
821 potential. *Cellular and Molecular Life Sciences.* 2016;73(5):901-22.
- 822 21. Meng X, Yang J, Dong M, Zhang K, Tu E, Gao Q, et al. Regulatory T cells in
823 cardiovascular diseases. *Nature Reviews Cardiology.* 2016;13(3):167-79.
- 824 22. Yodoi K, Yamashita T, Sasaki N, Kasahara K, Emoto T, Matsumoto T, et al. Foxp3+
825 regulatory T cells play a protective role in angiotensin II-induced aortic aneurysm
826 formation in mice. *Hypertension.* 2015;65(4):889-95.
- 827 23. Katsuki M, Hirooka Y, Kishi T, and Sunagawa K. Decreased proportion of Foxp3+ CD4+
828 regulatory T cells contributes to the development of hypertension in genetically
829 hypertensive rats. *J Hypertens.* 2015;33(4):773-83; discussion 83.
- 830 24. Barhoumi T, Kasal DA, Li MW, Shbat L, Laurant P, Neves MF, et al. T Regulatory
831 Lymphocytes Prevent Angiotensin II-Induced Hypertension and Vascular Injury.
832 *Hypertension.* 2011;57(3):469-76.
- 833 25. Kvakani H, Kleinewietfeld M, Qadri F, Park JK, Fischer R, Schwarz I, et al. Regulatory T
834 cells ameliorate angiotensin II-induced cardiac damage. *Circulation.* 2009;119(22):2904-
835 12.
- 836 26. Sanghavi M, and Rutherford JD. Cardiovascular Physiology of Pregnancy. *Circulation.*
837 2014;130(12):1003-8.
- 838 27. Osol G, and Mandala M. Maternal Uterine Vascular Remodeling During Pregnancy.
839 *Physiology (Bethesda, Md).* 2009;24:58-71.
- 840 28. Morton JS, Care AS, and Davidge ST. Mechanisms of Uterine Artery Dysfunction in
841 Pregnancy Complications. *Journal of Cardiovascular Pharmacology.* 2017;69(6):343-59.
- 842 29. Hemberger M, Hanna CW, and Dean W. Mechanisms of early placental development in
843 mouse and humans. *Nat Rev Genet.* 2020;21(1):27-43.
- 844 30. Burton GJ, Fowden AL, and Thornburg KL. Placental Origins of Chronic Disease.
845 *Physiological Reviews.* 2016;96(4):1509-65.
- 846 31. Cross JC, Hemberger M, Lu Y, Nozaki T, Whiteley K, Masutani M, and Adamson SL.
847 Trophoblast functions, angiogenesis and remodeling of the maternal vasculature in the
848 placenta. *Molecular and Cellular Endocrinology.* 2002;187(1):207-12.
- 849 32. Staff AC, Dechend R, and Pijnenborg R. Learning From the Placenta. *Hypertension.*
850 2010;56(6):1026-34.
- 851 33. Burton GJ, Woods AW, Jauniaux E, and Kingdom JCP. Rheological and physiological
852 consequences of conversion of the maternal spiral arteries for uteroplacental blood flow
853 during human pregnancy. *Placenta.* 2009;30(6):473-82.

- 854 34. Guimond M-J, Luross JA, Wang B, Terhorst C, Danial S, and Anne Croy B. Absence of
855 Natural Killer Cells during Murine Pregnancy is Associated with Reproductive
856 Compromise in TgE26 Mice1. *Biology of Reproduction*. 1997;56(1):169-79.
- 857 35. Gaynor LM, and Colucci F. Uterine natural killer cells: Functional distinctions and
858 influence on pregnancy in humans and mice. *Front Immunol*. 2017;8:467-.
- 859 36. Boulenouar S, Doisne J-M, Sferruzzi-Perri A, Gaynor LM, Kieckbusch J, Balmas E, et al.
860 The Residual Innate Lymphoid Cells in NFIL3-Deficient Mice Support Suboptimal
861 Maternal Adaptations to Pregnancy. *Front Immunol*. 2016;7(43).
- 862 37. Ashkar AA, Di Santo JP, and Croy BA. Interferon gamma contributes to initiation of
863 uterine vascular modification, decidual integrity, and uterine natural killer cell maturation
864 during normal murine pregnancy. *The Journal of experimental medicine*. 2000;192(2):259-
865 70.
- 866 38. Hazan AD, Smith SD, Jones RL, Whittle W, Lye SJ, and Dunk CE. Vascular-leukocyte
867 interactions: mechanisms of human decidual spiral artery remodeling in vitro. *Am J Pathol*.
868 2010;177(2):1017-30.
- 869 39. Felker AM, Chen Z, Foster WG, and Croy BA. Receptors for non-MHC ligands contribute
870 to uterine natural killer cell activation during pregnancy in mice. *Placenta*. 2013;34(9):757-
871 64.
- 872 40. Lima PDA, Tu MM, Rahim MMA, Peng AR, Croy BA, and Makrigiannis AP. Ly49
873 receptors activate angiogenic mouse DBA+ uterine natural killer cells. *Cellular &*
874 *Molecular Immunology*. 2014;11(5):467-76.
- 875 41. Guimond M-J, Wang B, and Croy BA. Engraftment of Bone Marrow from Severe
876 Combined Immunodeficient (SCID) Mice Reverses the Reproductive Deficits in Natural
877 Killer Cell-deficient tgε26 Mice. *The Journal of Experimental Medicine*. 1998;187(2):217.
- 878 42. Koopman LA, Kopcow HD, Rybalov B, Boyson JE, Orange JS, Schatz F, et al. Human
879 decidual natural killer cells are a unique NK cell subset with immunomodulatory potential.
880 *J Exp Med*. 2003;198(8):1201-12.
- 881 43. Perez-Garcia V, Fineberg E, Wilson R, Murray A, Mazzeo CI, Tudor C, et al. Placentation
882 defects are highly prevalent in embryonic lethal mouse mutants. *Nature*.
883 2018;555(7697):463-8.
- 884 44. Samstein RM, Arvey A, Josefowicz SZ, Peng X, Reynolds A, Sandstrom R, et al. Foxp3
885 exploits a pre-existent enhancer landscape for regulatory T cell lineage specification. *Cell*.
886 2012;151(1):153-66.
- 887 45. Kim JM, Rasmussen JP, and Rudensky AY. Regulatory T cells prevent catastrophic
888 autoimmunity throughout the lifespan of mice. *Nat Immunol*. 2007;8(2):191-7.
- 889 46. Guerin LR, Moldenhauer LM, Prins JR, Bromfield JJ, Hayball JD, and Robertson SA.
890 Seminal Fluid Regulates Accumulation of FOXP3+ Regulatory T Cells in the
891 Preimplantation Mouse Uterus Through Expanding the FOXP3+ Cell Pool and CCL19-
892 Mediated Recruitment. *Biol Reprod*. 2011.
- 893 47. Woods L, Perez-Garcia V, and Hemberger M. Regulation of Placental Development and
894 Its Impact on Fetal Growth-New Insights From Mouse Models. *Front Endocrinol*
895 *(Lausanne)*. 2018;9:570.
- 896 48. Weiss JM, Bilate AM, Gobert M, Ding Y, Curotto de Lafaille MA, Parkhurst CN, et al.
897 Neuropilin 1 is expressed on thymus-derived natural regulatory T cells, but not mucosa-
898 generated induced Foxp3+ T reg cells. *The Journal of experimental medicine*.
899 2012;209(10):1723-42, s1.

- 900 49. Takahashi T, Tagami T, Yamazaki S, Uede T, Shimizu J, Sakaguchi N, et al. Immunologic
901 self-tolerance maintained by CD25(+)CD4(+) regulatory T cells constitutively expressing
902 cytotoxic T lymphocyte-associated antigen 4. *The Journal of experimental medicine*.
903 2000;192(2):303-10.
- 904 50. Zenclussen AC, Gerlof K, Zenclussen ML, Sollwedel A, Bertoja AZ, Ritter T, et al.
905 Abnormal T-cell reactivity against paternal antigens in spontaneous abortion: adoptive
906 transfer of pregnancy-induced CD4+CD25+ T regulatory cells prevents fetal rejection in a
907 murine abortion model. *Am J Pathol*. 2005;166(3):811-22.
- 908 51. Chen Z, Zhang J, Hatta K, Lima PD, Yadi H, Colucci F, et al. DBA-lectin reactivity defines
909 mouse uterine natural killer cell subsets with biased gene expression. *Biol Reprod*.
910 2012;87(4):81.
- 911 52. Zhang JH, Yamada AT, and Croy BA. DBA-lectin reactivity defines natural killer cells
912 that have homed to mouse decidua. *Placenta*. 2009;30(11):968-73.
- 913 53. Spits H, Artis D, Colonna M, Diefenbach A, Di Santo JP, Eberl G, et al. Innate lymphoid
914 cells — a proposal for uniform nomenclature. *Nature Reviews Immunology*.
915 2013;13(2):145-9.
- 916 54. Abel AM, Yang C, Thakar MS, and Malarkannan S. Natural Killer Cells: Development,
917 Maturation, and Clinical Utilization. *Front Immunol*. 2018;9:1869.
- 918 55. Narni-Mancinelli E, Chaix J, Fenis A, Kerdiles YM, Yessaad N, Reynders A, et al. Fate
919 mapping analysis of lymphoid cells expressing the Nkp46 cell surface receptor. *Proc Natl
920 Acad Sci U S A*. 2011;108(45):18324-9.
- 921 56. Ma S, Caligiuri MA, and Yu J. A four-stage model for murine natural killer cell
922 development in vivo. *Journal of Hematology & Oncology*. 2022;15(1):31.
- 923 57. Yadi H, Burke S, Madeja Z, Hemberger M, Moffett A, and Colucci F. Unique receptor
924 repertoire in mouse uterine NK cells. *J Immunol*. 2008;181(9):6140-7.
- 925 58. Filipovic I, Chiossone L, Vacca P, Hamilton RS, Ingegnere T, Doisne J-M, et al. Molecular
926 definition of group 1 innate lymphoid cells in the mouse uterus. *Nature Communications*.
927 2018;9(1):4492.
- 928 59. Ashburner M, Ball CA, Blake JA, Botstein D, Butler H, Cherry JM, et al. Gene ontology:
929 tool for the unification of biology. The Gene Ontology Consortium. *Nat Genet*.
930 2000;25(1):25-9.
- 931 60. Kanehisa M, Furumichi M, Sato Y, Kawashima M, and Ishiguro-Watanabe M. KEGG for
932 taxonomy-based analysis of pathways and genomes. *Nucleic Acids Res*.
933 2023;51(D1):D587-d92.
- 934 61. Milacic M, Beavers D, Conley P, Gong C, Gillespie M, Griss J, et al. The Reactome
935 Pathway Knowledgebase 2024. *Nucleic Acids Res*. 2024;52(D1):D672-d8.
- 936 62. Aubert A, Jung K, Hiroyasu S, Pardo J, and Granville DJ. Granzyme serine proteases in
937 inflammation and rheumatic diseases. *Nat Rev Rheumatol*. 2024;20(6):361-76.
- 938 63. Froelich CJ, Pardo J, and Simon MM. Granule-associated serine proteases: granzymes
939 might not just be killer proteases. *Trends Immunol*. 2009;30(3):117-23.
- 940 64. Nüssing S, Sutton VR, Trapani JA, and Parish IA. Beyond target cell death - Granzyme
941 serine proteases in health and disease. *Mol Aspects Med*. 2022;88:101152.
- 942 65. Baldarelli RM, Smith CL, Ringwald M, Richardson JE, and Bult CJ. Mouse Genome
943 Informatics: an integrated knowledgebase system for the laboratory mouse. *Genetics*.
944 2024;227(1).

- 945 66. Jiang X, Wang Y, Xiao Z, Yan L, Guo S, Wang Y, et al. A differentiation roadmap of
946 murine placentation at single-cell resolution. *Cell Discov.* 2023;9(1):30.
- 947 67. Bettini M, and Vignali DA. Regulatory T cells and inhibitory cytokines in autoimmunity.
948 *Curr Opin Immunol.* 2009;21(6):612-8.
- 949 68. Khalil M, Wang D, Hashemi E, Terhune SS, and Malarkannan S. Implications of a 'Third
950 Signal' in NK Cells. *Cells.* 2021;10(8).
- 951 69. Saito S, Sakai M, Sasaki Y, Nakashima A, and Shiozaki A. Inadequate tolerance induction
952 may induce pre-eclampsia. *J Reprod Immunol.* 2007;76(1-2):30-9.
- 953 70. Robertson SA, Green ES, Care AS, Moldenhauer LM, Prins JR, Hull ML, et al. Therapeutic
954 Potential of Regulatory T Cells in Preeclampsia-Opportunities and Challenges. *Front*
955 *Immunol.* 2019;10:478-.
- 956 71. Burke SD, Barrette VF, Bianco J, Thorne JG, Yamada AT, Pang SC, et al. Spiral arterial
957 remodeling is not essential for normal blood pressure regulation in pregnant mice.
958 *Hypertension (Dallas, Tex : 1979).* 2010;55(3):729-37.
- 959 72. Elmore SA, Cochran RZ, Bolon B, Lubeck B, Mahler B, Sabio D, and Ward JM. Histology
960 Atlas of the Developing Mouse Placenta. *Toxicologic Pathology.* 2022;50(1):60-117.
- 961 73. Vacca P, Cantoni C, Vitale M, Prato C, Canegallo F, Fenoglio D, et al. Crosstalk between
962 decidual NK and CD14+ myelomonocytic cells results in induction of Tregs and
963 immunosuppression. *Proc Natl Acad Sci U S A.* 2010;107(26):11918-23.
- 964 74. Blois SM, Klapp BF, and Barrientos G. Decidualization and angiogenesis in early
965 pregnancy: unravelling the functions of DC and NK cells. *J Reprod Immunol.*
966 2011;88(2):86-92.
- 967 75. Stewart IJ, and Webster AJ. Lectin histochemical studies of mouse granulated metrial
968 gland cells. *The Histochemical Journal.* 1997;29(11):885-92.
- 969 76. Sojka DK, Yang L, Plougastel-Douglas B, Higuchi DA, Croy BA, and Yokoyama WM.
970 Cutting Edge: Local Proliferation of Uterine Tissue-Resident NK Cells during
971 Decidualization in Mice. *J Immunol.* 2018;201(9):2551-6.
- 972 77. Wang F, Qualls AE, Marques-Fernandez L, and Colucci F. Biology and pathology of the
973 uterine microenvironment and its natural killer cells. *Cellular & Molecular Immunology.*
974 2021;18(9):2101-13.
- 975 78. Nancy P, Tagliani E, Tay CS, Asp P, Levy DE, and Erlebacher A. Chemokine gene
976 silencing in decidual stromal cells limits T cell access to the maternal-fetal interface.
977 *Science.* 2012;336(6086):1317-21.
- 978 79. Moldenhauer LM, Diener KR, Hayball JD, and Robertson SA. An immunogenic
979 phenotype in paternal antigen-specific CD8(+) T cells at embryo implantation elicits later
980 fetal loss in mice. *Immunol Cell Biol.* 2017;95(8):705-15.
- 981 80. Foyle KL, and Robertson SA. Gamma delta (gammadelta) T cells in the female
982 reproductive tract: active participants or indifferent bystanders in reproductive success?
983 *Discov Immunol.* 2024;3(1):kyae004.
- 984 81. Tunster SJ, Watson ED, Fowden AL, and Burton GJ. Placental glycogen stores and fetal
985 growth: insights from genetic mouse models. *Reproduction.* 2020;159(6):R213-R35.
- 986 82. Lehtoranta L, Vuolteenaho O, Laine J, Polari L, Ekholm E, and Räsänen J. Placental
987 structural abnormalities have detrimental hemodynamic consequences in a rat model of
988 maternal hyperglycemia. *Placenta.* 2016;44:54-60.
- 989 83. Gewolb IH, Barrett C, and Warshaw JB. Placental growth and glycogen metabolism in
990 streptozotocin diabetic rats. *Pediatric research.* 1983;17(7):587-91.

991 84. Akison LK, Nitert MD, Clifton VL, Moritz KM, and Simmons DG. Review: Alterations
992 in placental glycogen deposition in complicated pregnancies: Current preclinical and
993 clinical evidence. *Placenta*. 2017;54:52-8.

994 85. Hanna J, Goldman-Wohl D, Hamani Y, Avraham I, Greenfield C, Natanson-Yaron S, et
995 al. Decidual NK cells regulate key developmental processes at the human fetal-maternal
996 interface. *Nat Med*. 2006;12(9):1065-74.

997 86. Sliz A, Locker KCS, Lampe K, Godarova A, Plas DR, Janssen EM, et al. Gab3 is required
998 for IL-2- and IL-15-induced NK cell expansion and limits trophoblast invasion during
999 pregnancy. *Sci Immunol*. 2019;4(38).

1000 87. Crespo Â C, van der Zwan A, Ramalho-Santos J, Strominger JL, and Tilburgs T. Cytotoxic
1001 potential of decidual NK cells and CD8+ T cells awakened by infections. *J Reprod
1002 Immunol*. 2017;119:85-90.

1003 88. Sen Santara S, Crespo Â C, Mulik S, Ovies C, Boulenouar S, Strominger JL, and
1004 Lieberman J. Decidual NK cells kill Zika virus-infected trophoblasts. *Proc Natl Acad Sci
1005 U S A*. 2021;118(47).

1006 89. Crespo Â C, Mulik S, Dotiwala F, Ansara JA, Sen Santara S, Ingersoll K, et al. Decidual
1007 NK Cells Transfer Granulysin to Selectively Kill Bacteria in Trophoblasts. *Cell*.
1008 2020;182(5):1125-39.e18.

1009 90. Vignali DAA, and Kuchroo VK. IL-12 family cytokines: immunological playmakers. *Nat
1010 Immunol*. 2012;13(8):722-8.

1011 91. Jia D, Jiang H, Weng X, Wu J, Bai P, Yang W, et al. Interleukin-35 Promotes Macrophage
1012 Survival and Improves Wound Healing After Myocardial Infarction in Mice. *Circulation
1013 Research*. 2019;124(9):1323-36.

1014 92. Xie Y, Zhang H, Huang J, and Zhang Q. Interleukin-35 in autoimmune dermatoses: Current
1015 concepts. *Open Medicine*. 2022;17(1):589-600.

1016 93. Shamji M, Layhadi J, Achkova D, Kouser L, Perera-Webb A, Couto Francisco N, et al.
1017 Role of Interleukin-35 in sublingual allergy immunotherapy. *Journal of Allergy and
1018 Clinical Immunology*. 2018;143.

1019 94. Cheng SB, and Sharma S. Interleukin-10: a pleiotropic regulator in pregnancy. *Am J
1020 Reprod Immunol*. 2015;73(6):487-500.

1021 95. Prins JR, Zhang B, Schjenken JE, Guerin LR, Barry SC, and Robertson SA. Unstable
1022 Foxp3+ regulatory T cells and altered dendritic cells are associated with
1023 lipopolysaccharide-induced fetal loss in pregnant interleukin 10-deficient mice. *Biol
1024 Reprod*. 2015;93(4):95.

1025 96. Murphy SP, Fast LD, Hanna NN, and Sharma S. Uterine NK Cells Mediate Inflammation-
1026 Induced Fetal Demise in IL-10-Null Mice. *The Journal of Immunology*. 2005;175(6):4084-
1027 90.

1028 97. Xu J, Wang Y, Jiang H, Sun M, Gao J, and Xie A. TGF- β in Mice Ameliorates
1029 Experimental Autoimmune Encephalomyelitis in Regulating NK Cell Activity. *Cell
1030 Transplantation*. 2019;28:096368971985235.

1031 98. Lazarova M, and Steinle A. Impairment of NKG2D-Mediated Tumor Immunity by TGF-
1032 β . *Front Immunol*. 2019;10:2689.

1033 99. Robertson A-KL, Rudling M, Zhou X, Gorelik L, Flavell RA, and Hansson GK. Disruption
1034 of TGF- β signaling in T cells accelerates atherosclerosis. *The Journal of Clinical
1035 Investigation*. 2003;112(9):1342-50.

1036 100. Pastrana JL, Sha X, Virtue A, Mai J, Cueto R, Lee IA, et al. Regulatory T cells and
1037 Atherosclerosis. *J Clin Exp Cardiol.* 2012;2012(Suppl 12):2.

1038 101. Foks A.C., and J. LAHK. Treating atherosclerosis with regulatory T cells. *Arteriosclerosis,
1039 Thrombosis, and Vascular Biology.* 2015;35(2):280-7.

1040 102. Mallat Z, Besnard S, Duriez M, Deleuze V, Emmanuel F, Bureau MF, et al. Protective role
1041 of interleukin-10 in atherosclerosis. *Circ Res.* 1999;85(8):e17-24.

1042 103. George J, Schwartzberg S, Medvedovsky D, Jonas M, Charach G, Afek A, and Shamiss
1043 A. Regulatory T cells and IL-10 levels are reduced in patients with vulnerable coronary
1044 plaques. *Atherosclerosis.* 2012;222(2):519-23.

1045 104. Ghiringhelli F, Ménard C, Martin F, and Zitvogel L. The role of regulatory T cells in the
1046 control of natural killer cells: relevance during tumor progression. *Immunol Rev.*
1047 2006;214:229-38.

1048 105. Kerdiles Y, Ugolini S, and Vivier E. T cell regulation of natural killer cells. *Journal of
1049 Experimental Medicine.* 2013;210(6):1065-8.

1050 106. Kurebayashi Y, Olkowski CP, Lane KC, Vasalatiy OV, Xu BC, Okada R, et al. Rapid
1051 Depletion of Intratumoral Regulatory T Cells Induces Synchronized CD8 T- and NK-cell
1052 Activation and IFN γ -Dependent Tumor Vessel Regression. *Cancer Res.*
1053 2021;81(11):3092-104.

1054 107. Samstein RM, Josefowicz SZ, Arvey A, Treuting PM, and Rudensky AY. Extrathymic
1055 generation of regulatory T cells in placental mammals mitigates maternal-fetal conflict.
1056 *Cell.* 2012;150(1):29-38.

1057 108. Williams PJ, Bulmer JN, Searle RF, Innes BA, and Robson SC. Altered decidual leucocyte
1058 populations in the placental bed in pre-eclampsia and foetal growth restriction: a
1059 comparison with late normal pregnancy. *Reproduction.* 2009;138(1):177-84.

1060 109. Milosevic-Stevanovic J, Krstic M, Radovic-Janosevic D, Popovic J, Tasic M, and Stojnev
1061 S. Number of decidual natural killer cells & macrophages in pre-eclampsia. *The Indian
1062 journal of medical research.* 2016;144(6):823-30.

1063 110. Stallmach T, Hebisch G, Orban P, and Lü X. Aberrant positioning of trophoblast and
1064 lymphocytes in the feto-maternal interface with pre-eclampsia. *Virchows Archiv.*
1065 1999;434(3):207-11.

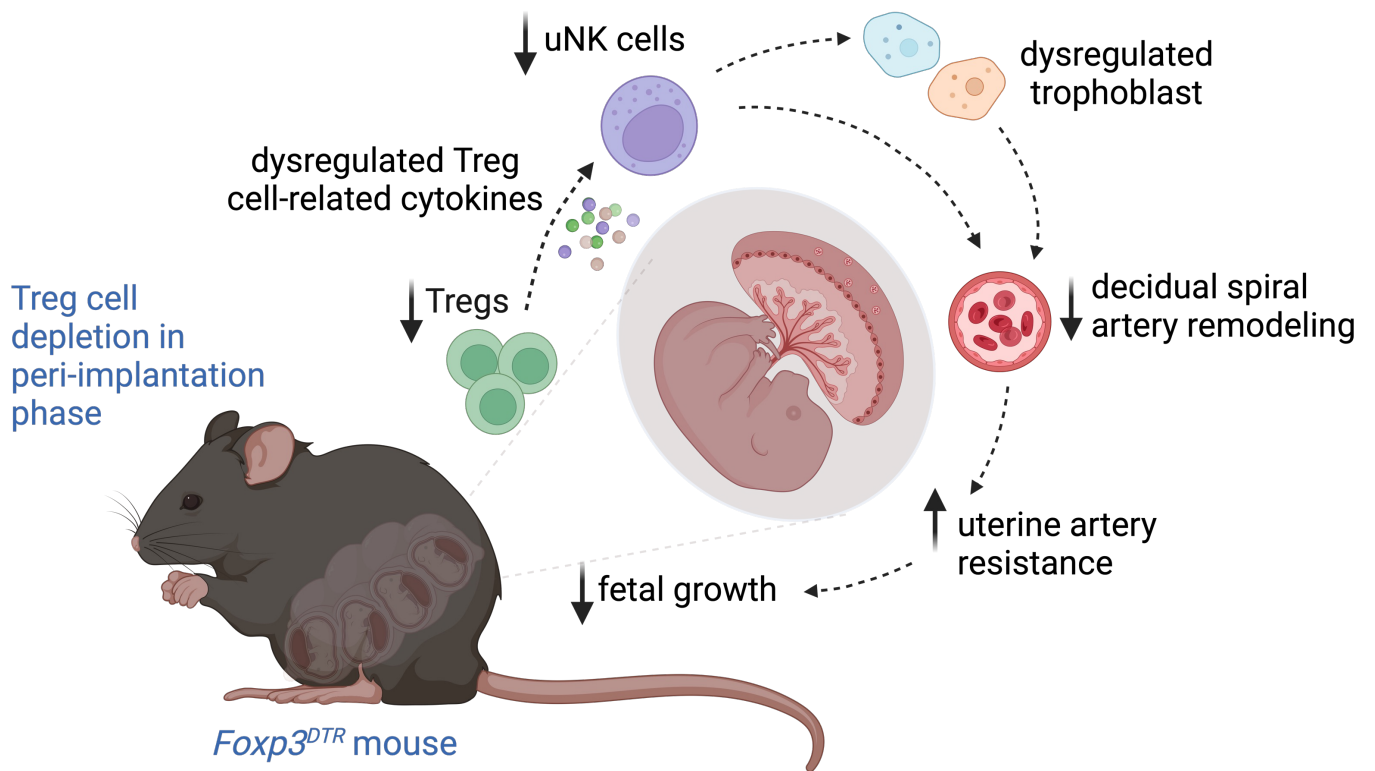
1066 111. Eide IP, Rolfseng T, Isaksen CV, Mecsei R, Roald B, Lydersen S, et al. Serious foetal
1067 growth restriction is associated with reduced proportions of natural killer cells in decidua
1068 basalis. *Virchows Archiv.* 2006;448(3):269-76.

1069 112. Dobin A, Davis CA, Schlesinger F, Drenkow J, Zaleski C, Jha S, et al. STAR: ultrafast
1070 universal RNA-seq aligner. *Bioinformatics.* 2013;29(1):15-21.

1071 113. Law CW, Chen Y, Shi W, and Smyth GK. voom: Precision weights unlock linear model
1072 analysis tools for RNA-seq read counts. *Genome Biol.* 2014;15(2):R29.

1073 114. Yu G, Wang L-G, Han Y, and He Q-Y. clusterProfiler: an R Package for Comparing
1074 Biological Themes Among Gene Clusters. *OMICS: A Journal of Integrative Biology.*
1075 2012;16(5):284-7.

1076



Graphical Abstract

Created with BioRender.com

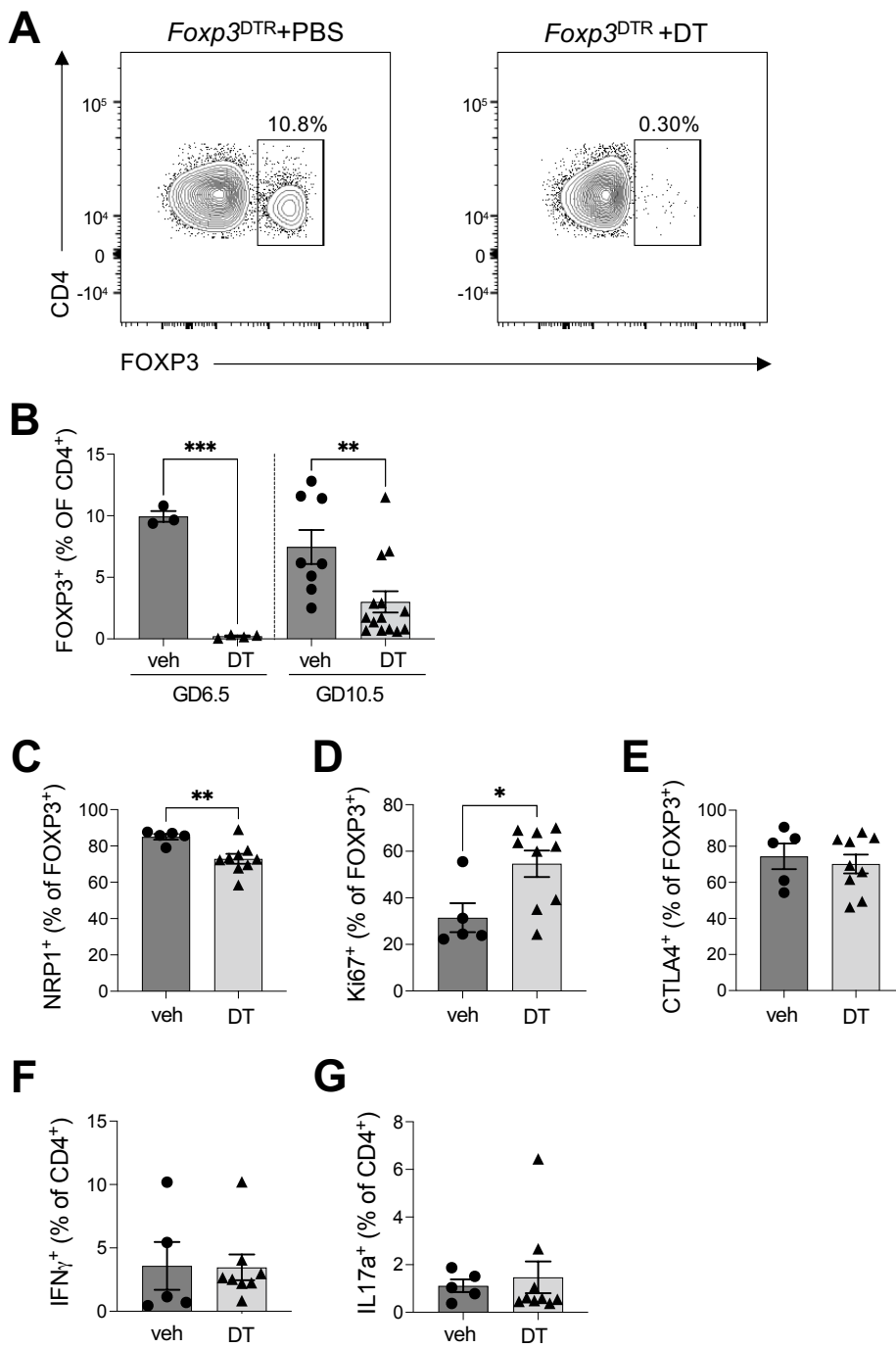
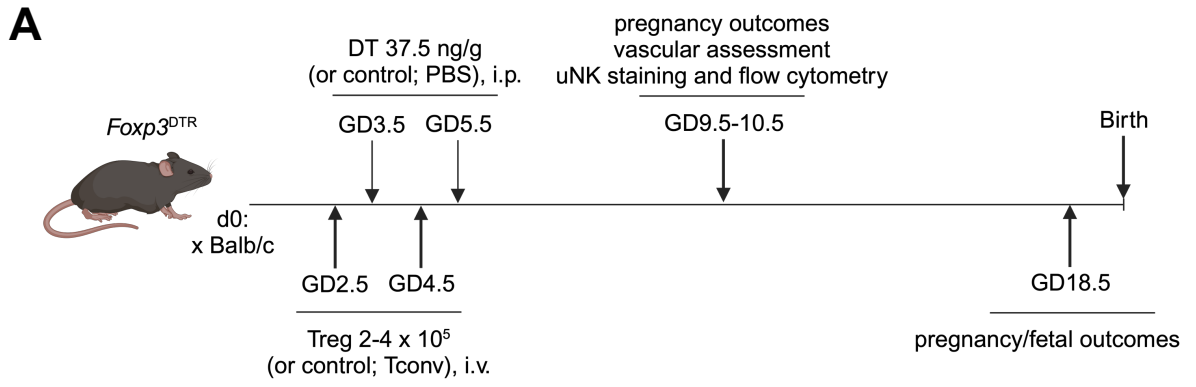
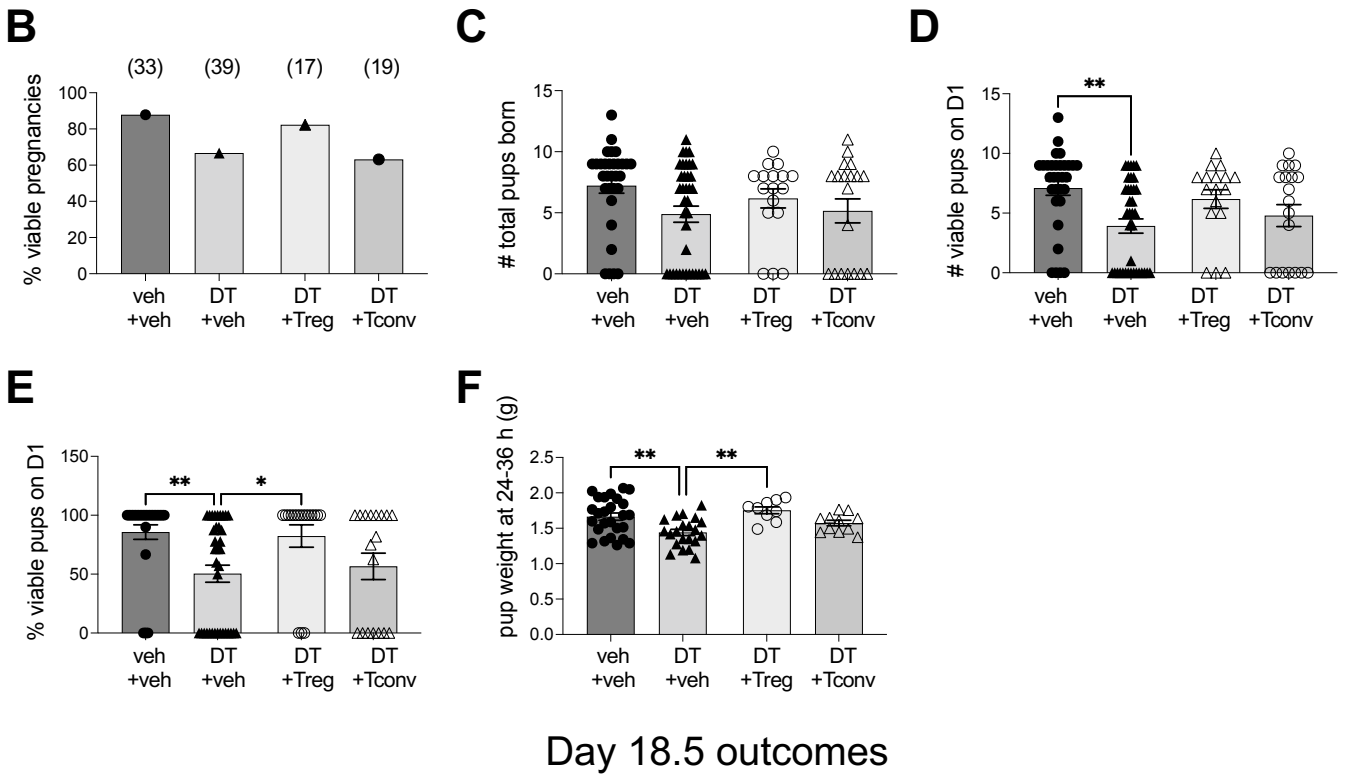


FIGURE 1



Birth outcomes



Day 18.5 outcomes

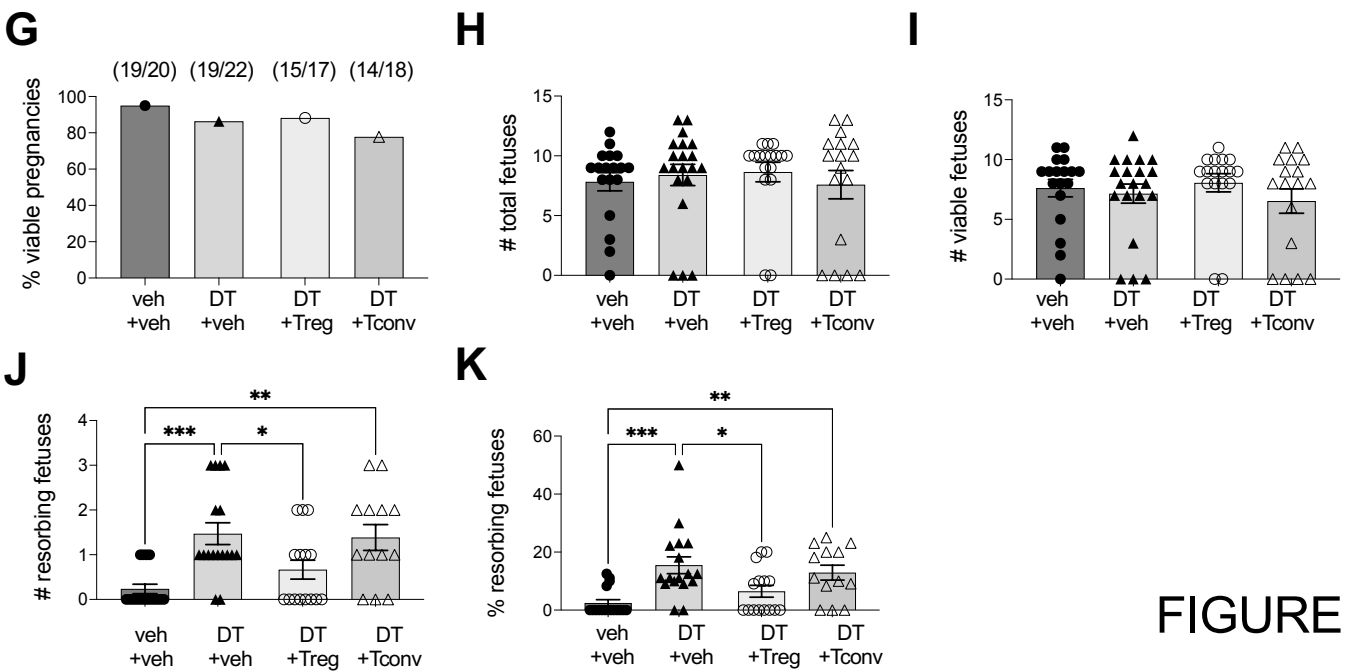


FIGURE 2

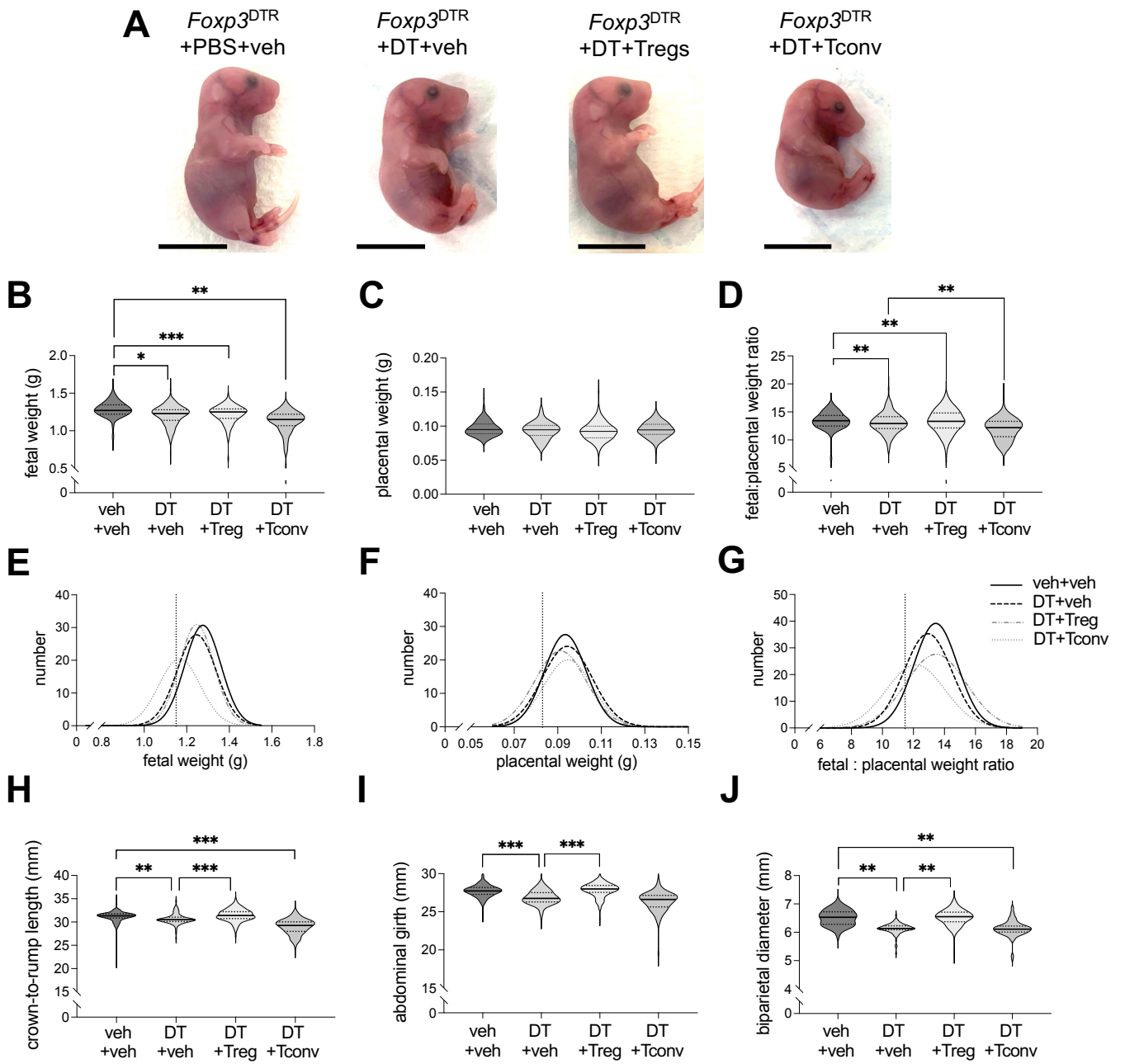


FIGURE 3

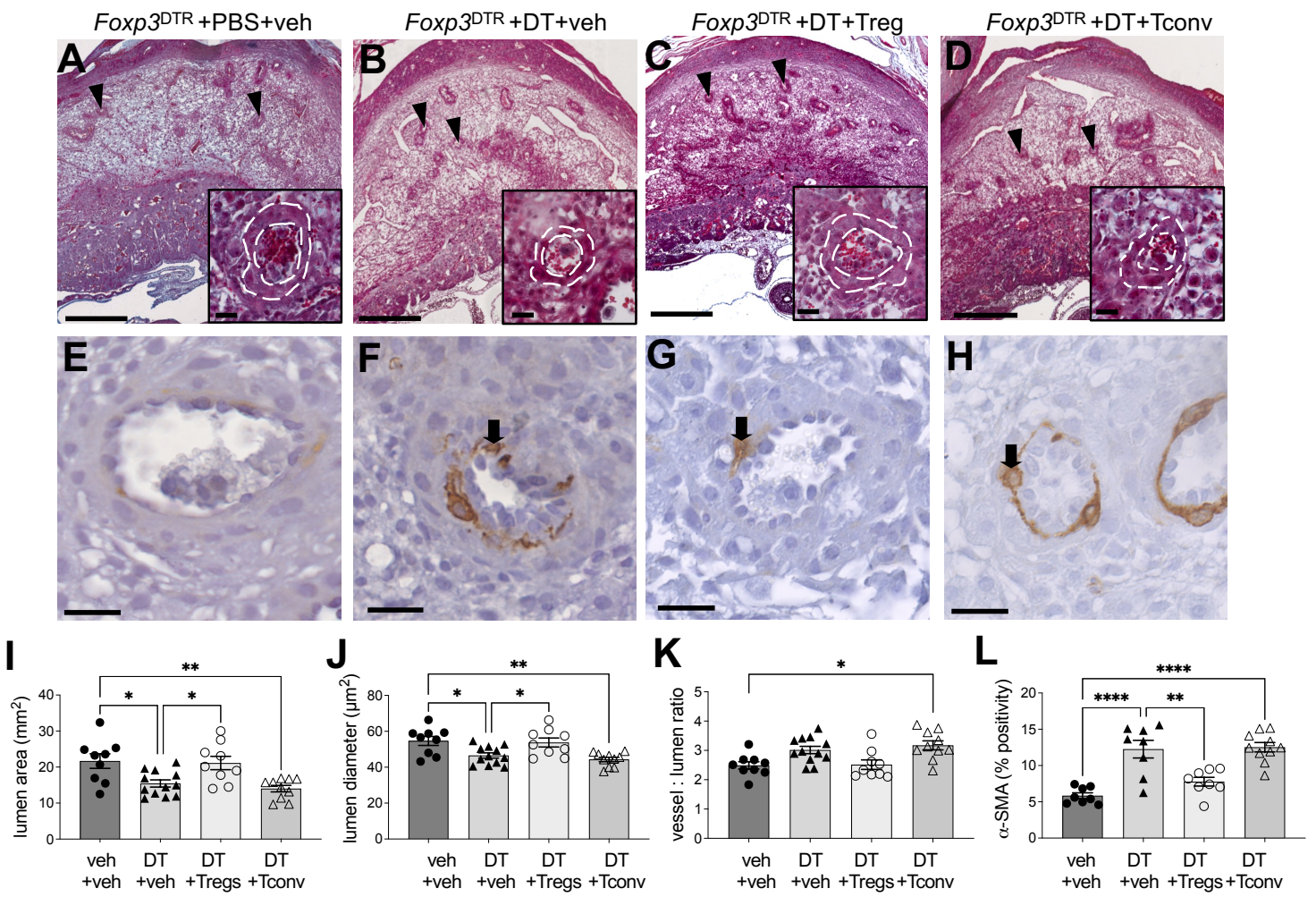


FIGURE 4

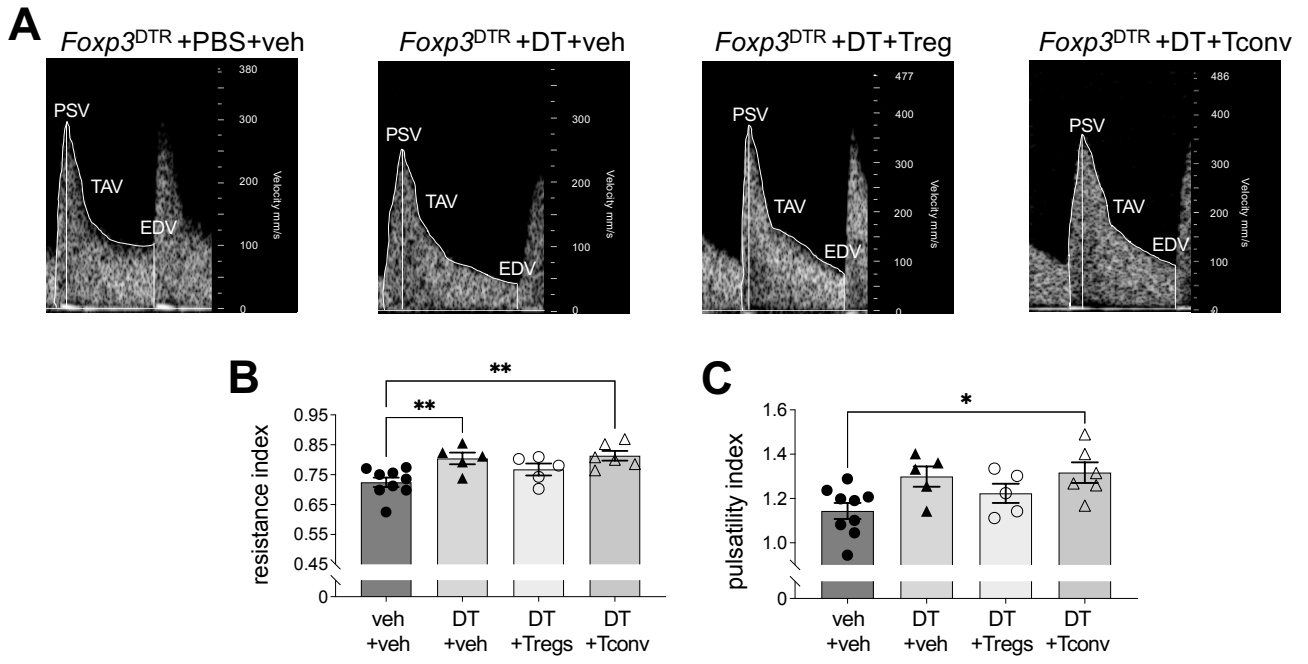


FIGURE 5

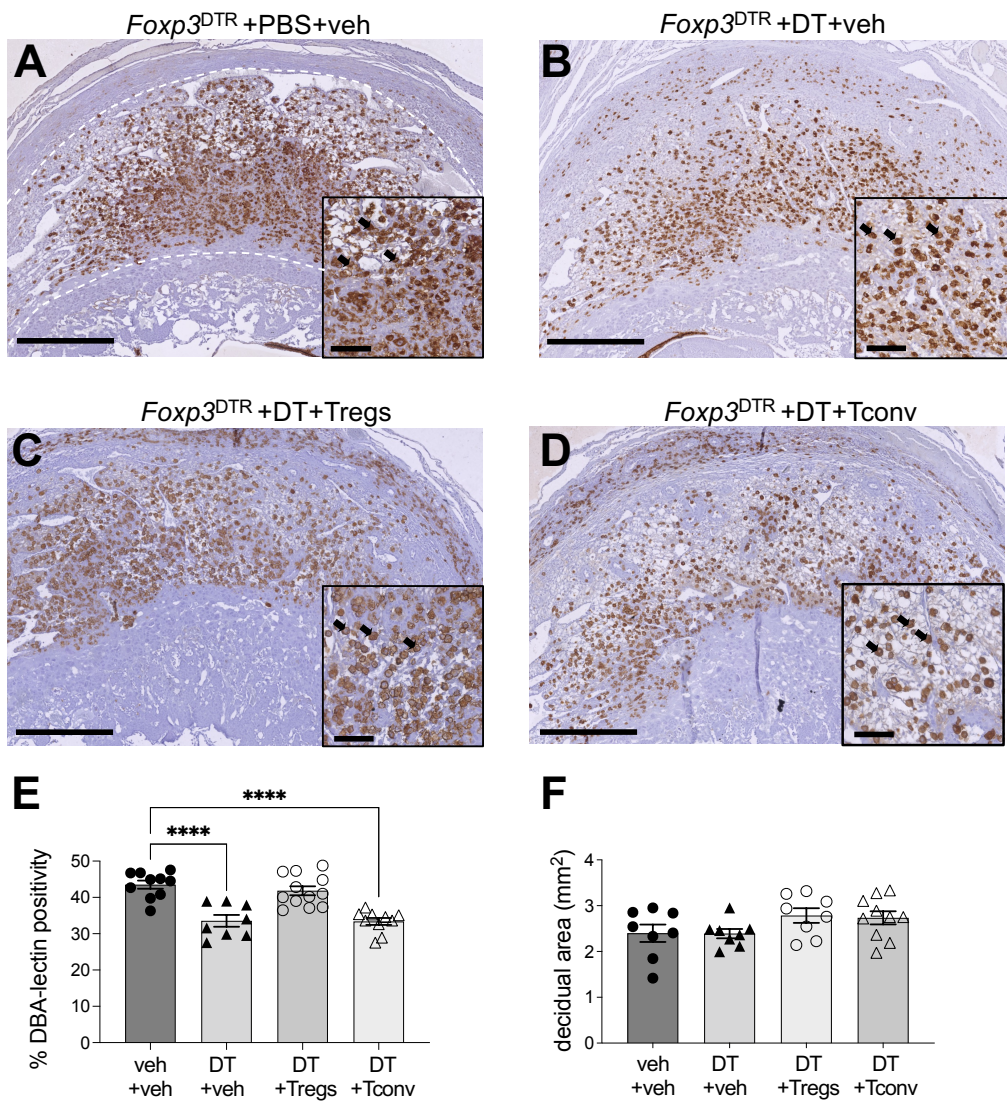
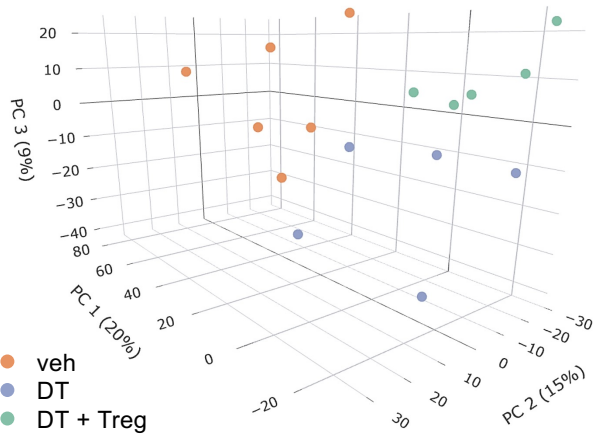
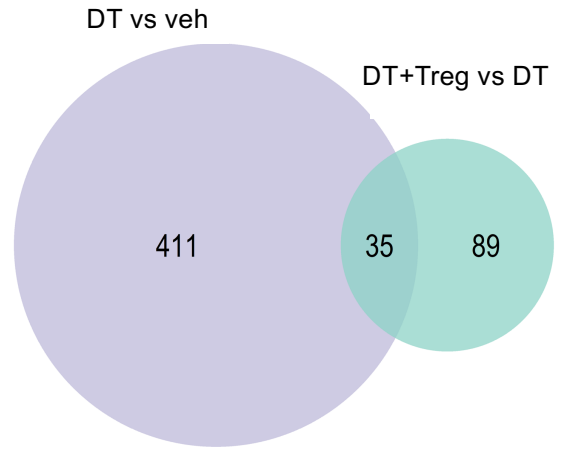
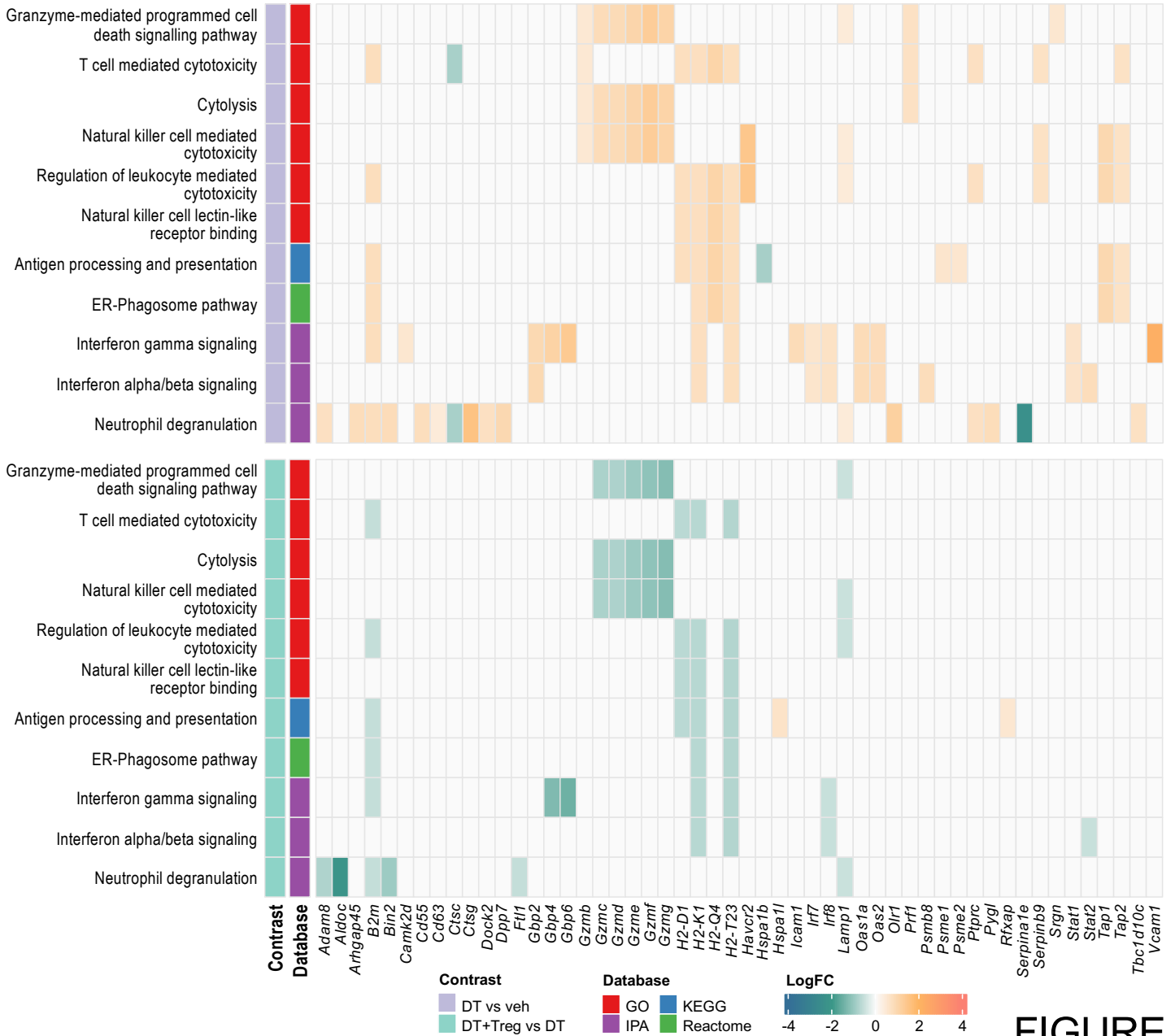


FIGURE 6

A**B****C****FIGURE 7**

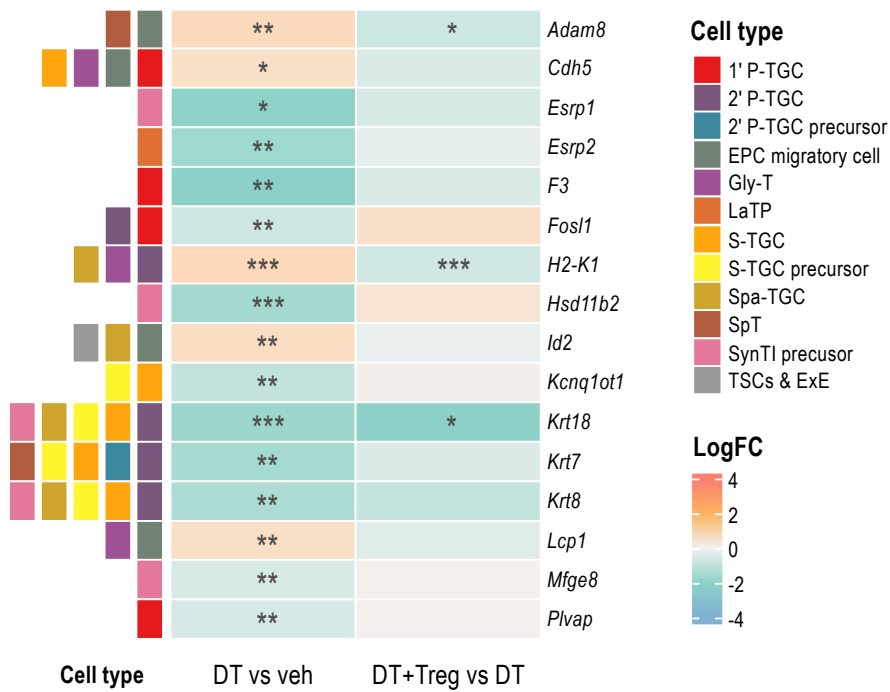


FIGURE 8

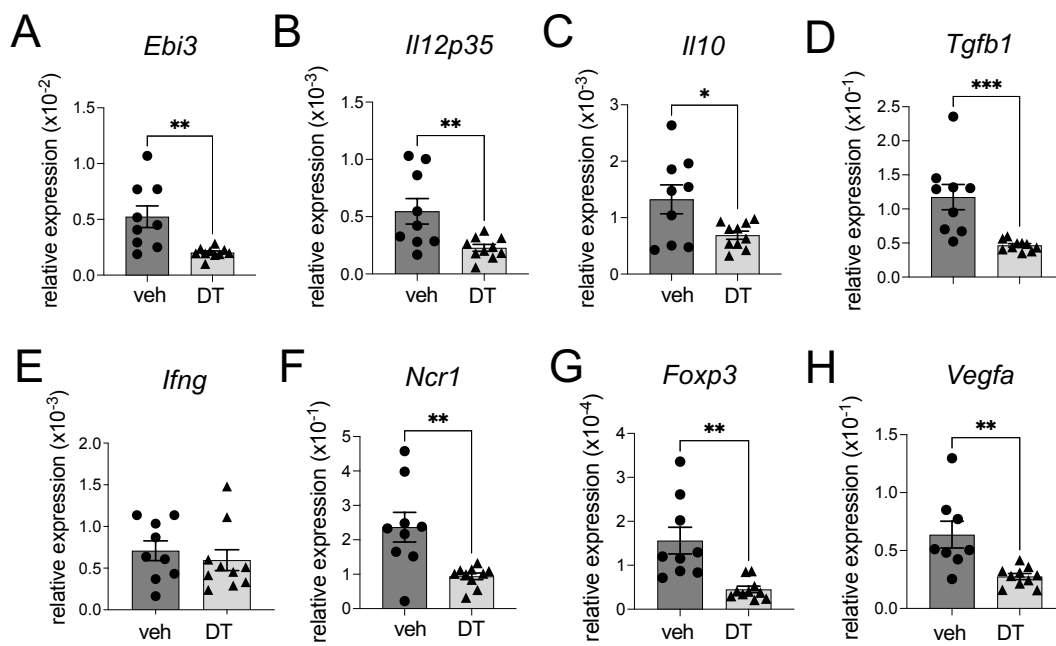
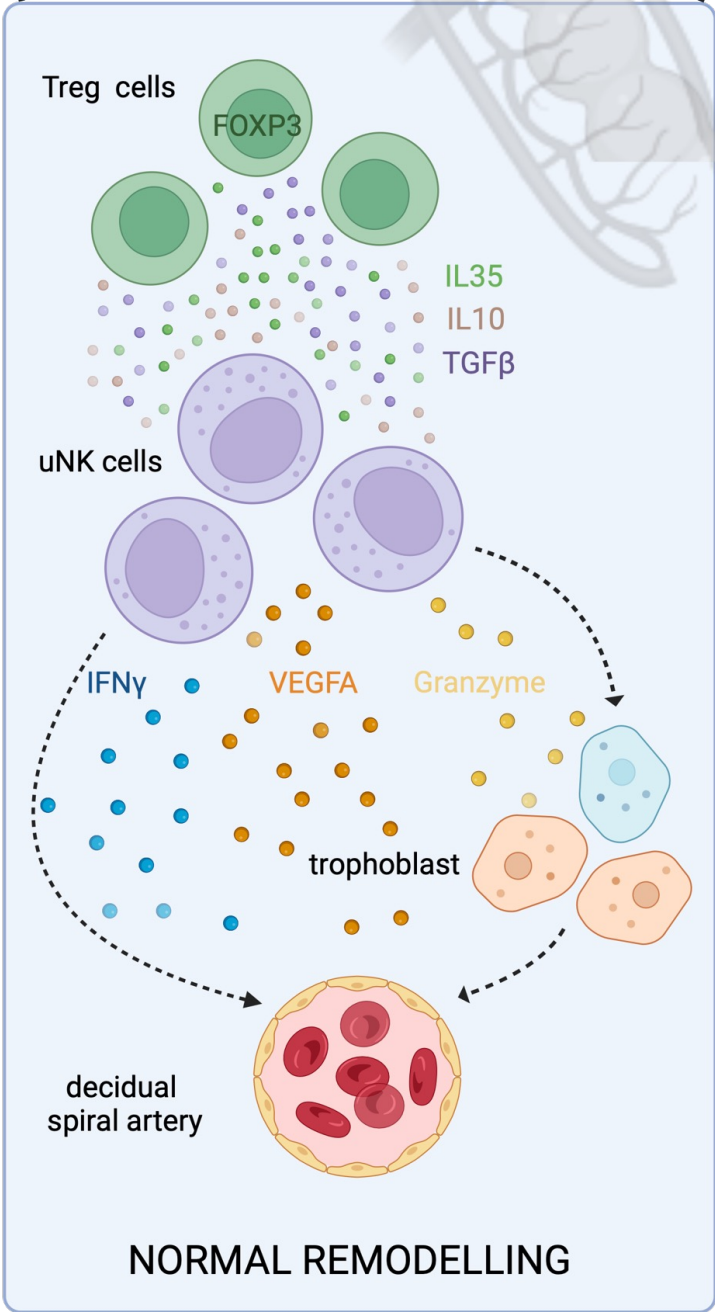
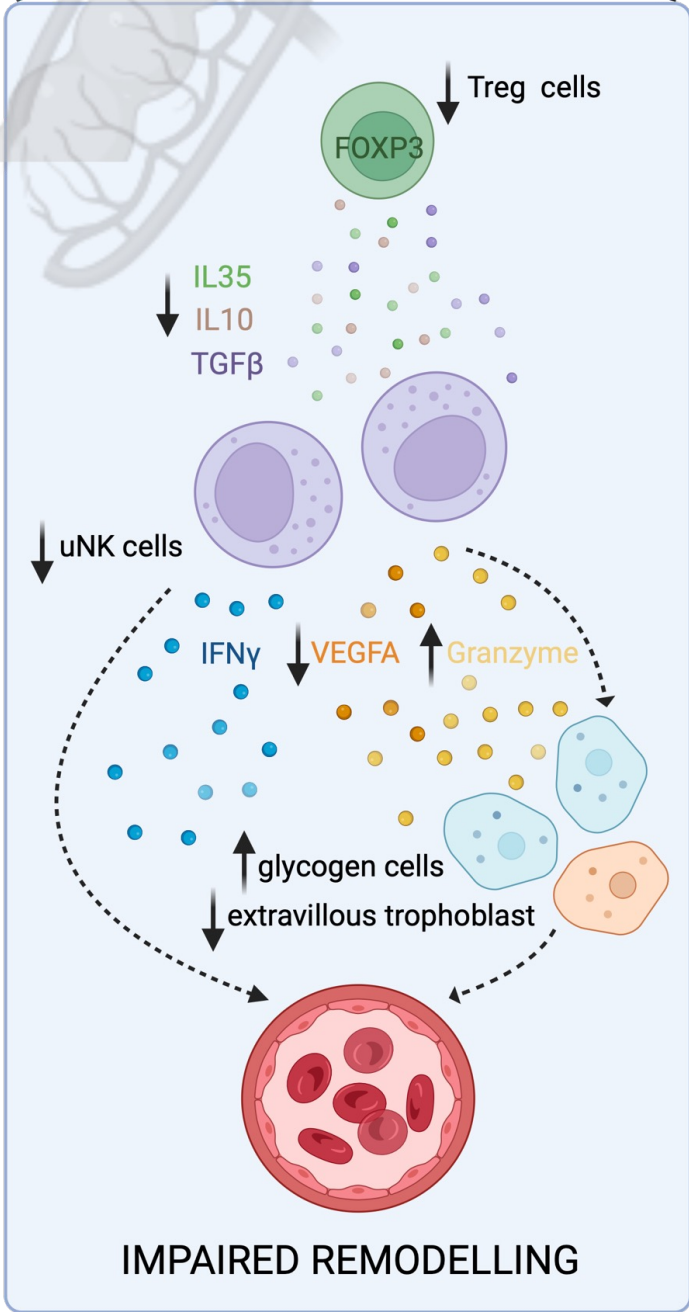


FIGURE 9

UTERUS



control



depleted of Treg cells

FIGURE 10